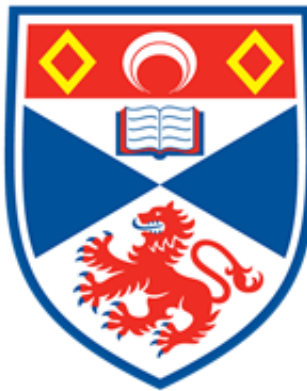


Time-splitting spectral methods for the Schrödinger equation in the semi-classical regime.

BSc Mathematics Final Project

Andrei Lazer



2025

I certify that this project report has been written by me, is a record of work carried out by me, and is essentially different from work undertaken for any other purpose or assessment.

Abstract

This project investigates the application of time-splitting spectral methods to numerically solve the time-dependent Schrödinger equation in the semi-classical regime, characterized by a small-scaled Planck constant ε . Heavily built upon and discussing results from Bao, Jin and Markowich 2002, we provide an analysis of these methods, including their derivation, numerical stability, and convergence properties. The study derives key theoretical results, such as the conservation of mass/total charge, order of convergence for the Lie and Strang splitting methods, and extends their application to two-dimensional problems. Through computational experimentation, we validate the theoretical findings, demonstrating the methods' ability to capture complex phenomena, such as caustics and singularities, with high accuracy for spatial and temporal step sizes of $\mathcal{O}(\varepsilon)$.

Acknowledgements

I would like to express my gratitude to my supervisor, Dr Irene Kyza. This project would not have been possible without her constant support. She helped me gain a strong foundation in numerical analysis, and gave me the freedom to explore the more physical and computational sides of the project.

I would also like to express my sincere gratitude to Sascha Schultz for generously offering his time, friendship, and mathematical advice. His support was both encouraging and instrumental throughout this project.

Finally, I would be remiss not to mention Raeann Lim, Nigel Lee, and Heather Thomson. I am thankful for their unwavering support, their patience in listening to my ramblings, and their comforting presence during countless hours in the library. Their company made this journey not only bearable but genuinely enjoyable.

Contents

| | | |
|----------|---|-----------|
| 1 | Introduction | 7 |
| 2 | The Schrödinger Equation | 8 |
| 2.1 | Quantum background for mathematicians | 8 |
| 2.2 | Notation, definitions & assumptions | 9 |
| 2.3 | Conservation of mass for the Schrödinger equation | 10 |
| 3 | Splitting methods for ODEs | 13 |
| 3.1 | General time splitting method | 14 |
| 3.2 | Lie splitting method | 17 |
| 3.3 | Strang splitting method | 18 |
| 3.4 | Experimental Order of Convergence | 19 |
| 4 | Semi-discretization | 21 |
| 4.1 | Operators for the splitting method | 21 |
| 4.2 | The Lie splitting method in the semi-discrete case | 23 |
| 4.3 | Lie splitting error for time-independent potentials | 24 |
| 4.4 | The Strang splitting method in the semi-discrete case | 26 |
| 5 | Spectral approximation | 28 |
| 5.1 | Fourier method | 28 |
| 5.2 | Lie splitting spectral method | 29 |
| 5.3 | Strang splitting spectral method | 33 |
| 5.4 | Extensions to d dimensions | 34 |
| 6 | Computational results | 36 |
| 6.1 | Numerical Examples | 36 |
| 6.2 | Experimental Order of Convergence | 40 |

| | |
|--|-----------|
| 7 Conclusions | 43 |
| A Mathematical derivations | 45 |
| A.1 An approach to the semi-classical scaling | 45 |
| A.2 Wigner functions and the free particle problem | 46 |
| B Computational implementation | 51 |
| B.1 Main functions | 51 |
| B.2 Experiments | 53 |

Chapter 1

Introduction

The Schrödinger equation is of great interest in Physics and Engineering, since it is used to model lasers, semiconductors, Bose-Einstein condensates [BT03], molecular dynamics and other physical problems with important quantum features. Here we will be concerned with the so-called semi-classical scaling of the equation, which is natural in many of these applications.

We are looking for a function $u(x, t)$ such that

$$i\varepsilon \frac{\partial u}{\partial t} + \frac{\varepsilon^2}{2} \frac{\partial^2 u}{\partial x^2} - V(x)u = 0,$$

with periodic spatial boundary conditions and a temporal initial condition. This is a linear, one-dimensional, initial-and-boundary value problem.

There are only a finite number of idealised physical states for which the equation above can be solved analytically, a few of which are explored in [GM97]. These systems are of great use when understanding quantum mechanics and the Schrödinger equation, but very often, numerical solutions are the only way forward.

At the same time, its numerical solution is challenging, because the solution $u(x, t)$ has oscillations of wavelength $\mathcal{O}(\varepsilon)$ in both time and space. This results in finite-difference methods such as the Crank-Nicholson method needing a spatial time step $h = o(\varepsilon)$ in order to resolve the oscillations. A family of methods that is known to perform well for problems of this form is the *time-splitting spectral methods*.

This project is based on, and will re-derive many of the results from [BJM02]. However, the aim is to present these results to an audience less familiar with numerical analysis and quantum mechanics.

In Chapter 2, we begin by introducing the Schrödinger equation and its semi-classical scaling, followed by conservation results that will inform the numerical methods discussed later. We then define general splitting methods and explore their associated convergence rates in Chapter 3. Chapter 4 follows by applying splitting methods to the semi-classical Schrödinger equation in the time domain, and Chapter 5 fully discretizes the method using a spectral method in space. Finally, in Chapter 6, we perform a series of computational experiments to validate the method's effectiveness and assess its order of convergence.

Chapter 2

The Schrödinger Equation

2.1 Quantum background for mathematicians

Quantum physics is a physical theory of atomic and sub-atomic particles. The fundamental difference between quantum and classical physics is that quantum physics can only give probabilities rather than exact predictions. This is often formulated in the language of *wave functions*.

The wave function ψ of a single non-relativistic quantum particle with mass m in a potential $V(x, t)$ follows the time-dependent Schrödinger equation (TDSE)

$$\frac{\hbar^2}{2m} \frac{\partial^2 \psi}{\partial x^2} + i\hbar \frac{\partial \psi}{\partial t} - V(x, t)\psi = 0. \quad (2.1)$$

Wave functions are auxiliary functions from which physical quantities called *observables*, such as position density, probability current, and energy, are calculated.

For example, the position density is defined as $n(x, t) = |\psi(x, t)|^2$, the squared modulus of the wave function. This is a probability density function for the position of the particle. We will also consider the current density, also known as the probability flux or probability current, $J(x, t) = \frac{\hbar}{m} \text{Im}(\overline{\psi(x, t)} \nabla \psi(x, t))$.

Since quantum physics governs the behaviour of very small things, then in order for this to be a physically consistent theory, we should expect that as mass and distance scales become large, a quantum system's behaviour will tend to that of its classical counterpart. It can be shown that an appropriate rescaling of variables is equivalent to $\hbar \rightarrow 0$.

The asymptotic treatment of the Schrödinger equation with $\hbar \rightarrow 0$ is known as "semi-classical", or the "semi-classical regime".

Sometimes this is called the WKB limit rather than the semi-classical limit, after the Wentzel–Kramers–Brillouin method used to derive asymptotics for the time-*independent* Schrödinger equation (TISE) in the semi-classical limit. See [Wil24, Chapter 5] for more information on this topic.

It can be shown that, through some rescalings of the space and time variables of the form $x \rightarrow Lx$ and $t \rightarrow \frac{L}{v}t$ for fixed positive parameters L and v , we can arrive at the semi-classical Schrödinger equation. See Appendix A.1 for further information on the derivation of the semi-classical Schrödinger equation.

We are looking for a function $u(x, t)$ with $x \in [a, b], t > 0$ such that

$$\left. \begin{array}{l} i\varepsilon \frac{\partial u}{\partial t} + \frac{\varepsilon^2}{2} \frac{\partial^2 u}{\partial x^2} - V(x)u = 0 \\ u(a, t) = u(b, t) \\ \frac{\partial u}{\partial x}(a, t) = \frac{\partial u}{\partial x}(b, t) \quad \forall t \\ u(x, t=0) = u_0(x) \end{array} \right\} t > 0, x \in [a, b]. \quad (2.2)$$

The small parameter ε is the (rescaled) Planck constant, V is a given scalar potential, u_0 is a given initial condition, and i denotes the complex unit ($i = \sqrt{-1}$). This is a linear one-dimensional initial value problem with periodic spatial boundary conditions.

2.2 Notation, definitions & assumptions

- We define $C^s(\mathbb{R})$ (C^s for simplicity), $s > 0$ as the set of all one-variable functions that are s times continuously differentiable in \mathbb{R} . $C(\mathbb{R})$ (C for simplicity) denotes the set of continuous functions on \mathbb{R} , while C^∞ is the set of infinitely differentiable functions on \mathbb{R} , also known as smooth functions. Similarly, we define $C^{s,r}$ when classifying multivariate functions.
- A function $v \in C^s(\mathbb{R})$ is called $(b-a)$ -periodic if $\frac{d^n v}{dx^n} \Big|_{x=a} = \frac{d^n v}{dx^n} \Big|_{x=b}$ for all $0 \leq n \leq s$. Note that $\frac{d^0 v}{dx^0} := v(x)$.
- For problem (2.2), we also assume the following:
 1. V and u_0 are C^∞ and $(b-a)$ -periodic.
 2. $u_0 : \mathbb{R} \rightarrow \mathbb{C}$.
 3. $V : \mathbb{R} \rightarrow \mathbb{R}^{\geq 0}$.

Furthermore, let $v, w \in C(\mathbb{R})$ be $(b-a)$ -periodic, complex-valued functions ($v, w : \mathbb{R} \rightarrow \mathbb{C}$). We define the L^2 inner product on (a, b) as:

$$\langle v, w \rangle = \int_a^b v(x) \overline{w}(x) dx, \quad (2.3)$$

where \overline{w} denotes the complex conjugate of w . The L^2 -norm of v on the interval (a, b) is defined as

$$\|v\|_{L^2} := \langle v, v \rangle^{\frac{1}{2}} = \left[\int_a^b |v(x)|^2 dx \right]^{\frac{1}{2}}.$$

Note:

- $\|v\|_{L^2}$ is always real, since the integrand $|v(x)|^2$ is non-negative and real everywhere.
- If $u = u(x, t)$, then $\|u\|_{L^2}$ is a univariate function of t , since the x dependence is “integrated out”.

2.3 Conservation of mass for the Schrödinger equation

It is clear that if the Schrödinger equation is a physical equation, it should follow some conservation of mass law. It will be useful to go through the general proof of conservation of mass since this will come up later when showing that splitting methods retain this invariance.

The conservation of mass for a quantum particle with wave function $u(x, t)$ is the honesty condition for its position density function, since if the mass is conserved, the particle must be somewhere. The p.d.f. of the position $n(x, t)$ is defined as

$$n(x, t) = \frac{d}{dx} \mathbb{P}(X \leq x) := |u(x, t)|^2 = u(x, t) \overline{u(x, t)},$$

for the random variable X , the position of the particle. Therefore, the honesty condition is equivalent to

$$\|u(x, t)\|_{L^2}^2 = 1 \quad \forall t.$$

Note that if u is a solution to (2.2), then so is any rescaling Au , so all we need to show is that $\frac{d}{dt} \|u(x, t)\|_{L^2}^2 = 0$, since we can always normalize our wave function later.

First, we will prove some auxiliary lemmas to help with the proof for conservation of mass.

Lemma 2.1. *Let $v \in C^{1,1}(\mathbb{R} \times \mathbb{R})$ ($v = v(x, t)$) be a $(b - a)$ -periodic function with respect to the spatial (first) variable. Then,*

$$\operatorname{Re} \int_a^b \bar{v}(x, t) \frac{\partial v}{\partial t} dx = \frac{1}{2} \frac{d}{dt} \|v(t)\|_{L^2}^2.$$

Proof. We first have that for all $z \in \mathbb{C}$,

$$\operatorname{Re}(z) = \frac{1}{2}(z + \bar{z}).$$

Therefore, since complex conjugation commutes with differentiation, integration and multiplication,

$$\begin{aligned} \operatorname{Re} \int_a^b \bar{v}(x, t) \frac{\partial v}{\partial t} dx &= \frac{1}{2} \left(\int_a^b \bar{v}(x, t) \frac{\partial v}{\partial t} dx + \int_a^b v(x, t) \frac{\partial \bar{v}}{\partial t} dx \right) \\ &= \frac{1}{2} \int_a^b \bar{v}(x, t) \frac{\partial v}{\partial t} + v(x, t) \frac{\partial \bar{v}}{\partial t} dx \\ &= \frac{1}{2} \int_a^b \frac{\partial}{\partial t} [v(x, t) \bar{v}(x, t)] dx. \end{aligned}$$

The final step follows by the product rule. Now, since t is independent of x , and our integrand is bounded and continuous, we have that

$$\operatorname{Re} \int_a^b \bar{v}(x, t) \frac{\partial v}{\partial t} dx = \frac{1}{2} \frac{d}{dt} \int_a^b v(x, t) \bar{v}(x, t) dx.$$

Therefore,

$$\operatorname{Re} \int_a^b \bar{v}(x, t) \frac{\partial v}{\partial t} dx = \frac{1}{2} \frac{d}{dt} \|v(t)\|_{L^2}^2.$$

□

Lemma 2.2. *Let $v \in C^2$ be $(b-a)$ -periodic in x . Then,*

$$\int_a^b \frac{d^2 v(x)}{dx^2} \bar{v}(x) dx = - \left\| \frac{dv}{dx} \right\|_{L^2}^2 \in \mathbb{R}.$$

Proof. Using integration by parts,

$$\int_a^b \frac{d^2 v(x)}{dx^2} \bar{v}(x) dx = \frac{dv(x)}{dx} \bar{v}(x) \Big|_a^b - \int_a^b \frac{dv(x)}{dx} \frac{d\bar{v}(x)}{dx} dx.$$

Since v is $(b-a)$ -periodic, so are $\frac{dv(x)}{dx}$ and $\bar{v}(x)$, so the first term on the right hand side cancels to 0.

$$\int_a^b \frac{d^2 v(x)}{dx^2} \bar{v}(x) dx = - \int_a^b \frac{dv(x)}{dx} \frac{d\bar{v}(x)}{dx} dx = - \left\| \frac{dv}{dx} \right\|_{L^2}^2$$

□

Theorem 2.1. *For a solution $u(x, t)$ of (2.2),*

$$\|u(t)\|_{L^2} = \|u_0\|_{L^2}$$

Proof. Multiplying (2.2) by $-i\bar{u}$, we get

$$\varepsilon \frac{\partial u}{\partial t} \bar{u} - \frac{i\varepsilon^2}{2} \frac{\partial^2 u}{\partial x^2} \bar{u} + iV(x)u\bar{u} = 0.$$

Now, we integrate with respect to x ,

$$\varepsilon \int_a^b \frac{\partial u}{\partial t} \bar{u} dx - \frac{i\varepsilon^2}{2} \int_a^b \frac{\partial^2 u}{\partial x^2} \bar{u} dx + i \int_a^b V(x)u\bar{u} dx = 0.$$

Finally, taking real parts,

$$\varepsilon \operatorname{Re} \left(\int_a^b \frac{\partial u}{\partial t} \bar{u} dx \right) - \frac{\varepsilon^2}{2} \operatorname{Re} \left(i \int_a^b \frac{\partial^2 u}{\partial x^2} \bar{u} dx \right) + \operatorname{Re} \left(i \int_a^b V(x) u \bar{u} dx \right) = 0.$$

We can look at the three terms one by one:

- By Lemma 2.1:

$$\operatorname{Re} \left(\int_a^b \frac{\partial u}{\partial t} \bar{u} dx \right) = \frac{1}{2} \frac{d}{dt} \|u(t)\|_{L^2}^2$$

- By Lemma 2.2:

$$\operatorname{Re} \left(i \int_a^b \frac{\partial^2 u}{\partial x^2} \bar{u} dx \right) = \operatorname{Re} \left(-i \left\| \frac{\partial u}{\partial t} \right\|_{L^2}^2 \right) = 0,$$

since the L_{L^2} norm defined in (2.3) is always real.

- The final integrand is a product of two real values: $V(x)$ and $u \bar{u} = |u(x, t)|^2$, so

$$\operatorname{Re} \left(i \int_a^b V(x) u \bar{u} dx \right) = 0.$$

Therefore, substituting our results in, it follows that

$$\begin{aligned} \varepsilon \frac{1}{2} \frac{d}{dt} \|u(t)\|_{L^2}^2 &= 0 \\ \frac{d}{dt} \|u(t)\|_{L^2} &= 0 \\ \|u(t)\|_{L^2} &= C \\ \|u(t)\|_{L^2} &= \|u(0)\|_{L^2} \\ \|u(t)\|_{L^2} &= \|u_0\|_{L^2}. \end{aligned}$$

□

Remark 2.1. This result is often also called conservation of total charge [BJM02; BJM03] since the charge density is defined to be proportional to the position density

$$\rho_q(x, t) := q|u(x, t)|^2 = qn(x, t).$$

Therefore, conservation of mass implies conservation of total charge.

Chapter 3

Splitting methods for ODEs

Splitting methods are a type of numerical integration method which seeks to approximate a dynamical system by splitting it into simpler parts.

For example, suppose we seek to solve the linear first-order dynamical system

$$\frac{dx}{dt} = f(x) \quad (3.1)$$

with $f(x)$ not simply integrable w.r.t. time, t . A splitting method assumes a decomposition of f into $f(x) = f_1(x) + f_2(x)$, where each of the differential equations

$$\frac{dx}{dt} = f_1(x) \quad (3.2)$$

and

$$\frac{dx}{dt} = f_2(x) \quad (3.3)$$

can be solved either analytically, or using higher order methods than f .

In an effort to sketch out a splitting method, suppose we want to integrate (3.1) from t^n to t^{n+1} in one step, where $x^n = x(t^n)$ is known.

First, we start at (t^n, x^n) and solve the IVP given by (3.2)

$$\frac{dx_1}{dt} = f_1(x), \quad x_1(t^n) = x^n$$

for $x^* = x_1(t^{n+1})$. This takes us to a point x^* . Then, we solve the second IVP given by (3.3) from x^*

$$\frac{dx_2}{dt} = f_2(x), \quad x_2(t^n) = x^*.$$

Our splitting estimate for $x^{n+1} \approx x(t^{n+1})$ is $x^{n+1} = x_2(t^{n+1})$.

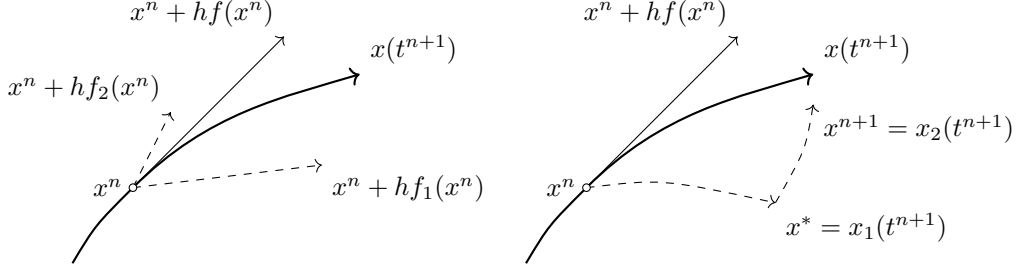


Figure 3.1: An approximation to the solution is obtained by stepping through f_1 's solution, then f_2 's.
Recreated from [Fra08, Chapter 13].

Splitting methods are not limited to one-dimensional differential equations, nor to a separation into only two parts. The following section describes the general time splitting method for any number of sub-problems.

3.1 General time splitting method

Consider the following linear first-order ODE:

$$\left. \begin{aligned} \frac{dx}{dt} &= \mathbf{C}x(t) \\ x(0) &= x_0 \end{aligned} \right\} t \in (0, T] \quad (3.4)$$

for $T > 0$, and \mathbf{C} a constant linear operator with respect to t . $x(t)$ is left ambiguous in order for the splitting methods in this chapter to be as general as possible. At separate points in this work, $x(t)$ is both a finite-dimensional vector in \mathbb{C}^n , as well as a function in L^2 .

Lemma 3.1. *The exact solution to (3.4) is as follows:*

$$x(t) = e^{\mathbf{C}t}x_0$$

Proof. This can be shown by differentiating both sides of (3.1) with respect to t , bearing in mind the generalized exponential function

$$e^{\mathbf{C}t} := \sum_{n=0}^{\infty} \frac{(\mathbf{C}t)^n}{n!} = \mathbf{I} + \mathbf{C}t + \frac{(\mathbf{C}t)^2}{2!} + \dots$$

and that exponentiation of operators is defined as repeated application. \square

We will now look at how to approximate this solution on a partition of $[0, T]$, $0 =: t^0 < t^1 < \dots < t^N := T$. Let x^n be defined as the approximation of $x(t^n)$.

Consider the ODE on the subinterval $(t^n, t^{n+1}]$, $n = 0, 1, \dots, N - 1$:

$$\left. \begin{aligned} \frac{dx}{dt} &= \mathbf{C}x(t) \\ x(0) &= x_0 \end{aligned} \right\}$$

Suppose we have $\mathbf{C}_i, i = 1, 2, \dots, P \in \mathbb{N}$ such that

$$\mathbf{C} = \sum_{i=1}^P \mathbf{C}_i.$$

Then, we can approximate the exact solution as follows:

for $n = 0, 1, \dots, N$:

First solve

$$\left. \begin{aligned} \frac{dx_1}{dt} &= \mathbf{C}_1 x_1(t) \\ x_1(t^n) &= x^n \end{aligned} \right\} \quad (3.5)$$

and then for $i = 2, 3, \dots, P$, we solve

$$\left. \begin{aligned} \frac{dx_i}{dt} &= \mathbf{C}_i x_i(t) \\ x_i(t^n) &= x_{i-1}(t^{n+1}) \end{aligned} \right\} \quad (3.6)$$

The approximation of x^{n+1} is the solution of (3.6) at $i = P, t = t^{n+1}$.

Using Lemma 3.1 and induction on P , we obtain the following solutions for (3.5) and (3.6)

$$\begin{aligned} x_1(t) &= e^{(t-t^n)\mathbf{C}_1} x^n, \\ x_i(t) &= e^{(t-t^n)\mathbf{C}_i} e^{k\mathbf{C}_{i-1}} \cdots e^{k\mathbf{C}_1} x^n, \end{aligned} \quad (3.7)$$

where $t \in (t^n, t^{n+1}]$.

Lemma 3.2. *The local approximation x^{n+1} of $x(t^{n+1})$ in terms of x^n yielded by the general splitting method is:*

$$x^{n+1} = \left(\prod_{n=1}^P e^{k\mathbf{C}_n} \right) x^n$$

Proof. This can be shown by substituting $i = P$ and $t = t^{n+1}$ into (3.7). \square

A natural next question is to ask when this is an exact method. To investigate this, we must first show an auxiliary result.

Lemma 3.3. *For a and b which need not commute,*

$$ab = ba \Rightarrow e^a e^b = e^{a+b}$$

Proof. The Baker-Campbell-Haussdorf theorem [Eur] gives the solution c to the equation $e^c = e^a e^b$ as

$$c = a + b + \frac{1}{2}[a, b] + \frac{1}{12}[a, [a, b]] + \dots$$

for $[a, b] = ab - ba$ the commutator of a and b . “ \dots ” indicates higher order nestings of commutators of a and b . More simply, we can write

$$c = a + b + D(a, b)$$

where $D = 0$ if $[a, b] = 0$.

So,

$$\begin{aligned} e^a e^b - e^{a+b} &= e^c - e^{a+b} \\ &= \sum_{n=0}^{\infty} \frac{(a+b)^n}{n!} - \frac{c^n}{n!} \\ &= \sum_{n=0}^{\infty} \frac{(a+b)^n - [a+b+D(a,b)]^n}{n!}. \end{aligned}$$

So if $ab = ba$, $D(a, b) = 0$, then the summand above is identically 0 for all n , and we obtain the statement of Lemma 3.3.

□

This result is an important one, since we cannot assume the usual identity $e^a e^b = e^{a+b}$ for non-commutative algebras.

We can now show when a splitting method is exact. For an exact method, we have that the truncation error $T_{n+1} = 0 \forall n$. So,

$$\begin{aligned} x^{n+1} &= x(t^{n+1}) \\ \left(\prod_{n=1}^P e^{k\mathbf{C}_n} \right) x^n &= e^{k\mathbf{C}} x^n \quad \forall x^n \\ \prod_{j=1}^P e^{k\mathbf{C}_j} &= e^{k\mathbf{C}} \\ \prod_{j=1}^P e^{k\mathbf{C}_j} &= e^{k(\mathbf{C}_1 + \dots + \mathbf{C}_P)}. \end{aligned}$$

Using Lemma 3.3 and induction on P , we get that if all of $\mathbf{C}_1, \mathbf{C}_2, \dots, \mathbf{C}_P$ commute with each other, then this is an exact method. This is not necessarily the case for all linear operators, and is definitely not the case for the differential operators we need to use for the Schrödinger equation.

Intuitively, this dependence on the commutator makes sense. A splitting method essentially reorders the integration of a dynamical system and assumes we can step through each operator in series. This reordering assumption should only work if our operators commute.

Visually, if the operators \mathbf{C}_i commute, x^{n+1} will coincide with $x(t^{n+1})$ in Figure 3.1. Otherwise, we'll see the gap shown in the figure, the size of which is equal to the splitting error.

3.2 Lie splitting method

In this work, we will consider two splitting methods: the Lie and Strang splitting methods. Note that in other works, such as [BJM02], these methods are referred to as SP1 and SP2 respectively.

In this section, we leave $x(t)$ to be an indeterminate member of some vector space. Later on in this project, $x(t)$ could be a function of spatial variables, or a finite-dimensional vector. The notation $\|x(t)\|_2$ below refers to both the ℓ^2 -norm for finite-dimensional vectors

$$\|x(t)\|_{\ell^2}^2 = \frac{1}{M} \sum_i [x_i(t)]^2$$

and the L^2 -norm for functions

$$\|x(t)\|_{L^2}^2 = \int_a^b [x(t)]^2 dx$$

depending on the form of $x(t)$. This only works in this section because all we assume about $\|\cdot\|_2$ is the triangle inequality and non-negativity, conditions which hold for all norms.

Consider now the problem

$$\begin{cases} \frac{dx}{dt} = (\mathbf{A} + \mathbf{B})x(t), & t \in (t^n, t^{n+1}] \\ x(t^n) = x^n \end{cases} \quad (3.8)$$

Where \mathbf{A} and \mathbf{B} are linear operators. The *Lie splitting method* is a special case of the general splitting method described in (3.5) and (3.6), with $P = 2$, $\mathbf{C}_1 = \mathbf{A}$, and $\mathbf{C}_2 = \mathbf{B}$.

Using (3.4) and (3.7), we obtain

$$\begin{aligned} x(t) &= e^{t(\mathbf{A}+\mathbf{B})} \\ x^{n+1} &= e^{k\mathbf{A}} e^{k\mathbf{B}} x^n. \end{aligned}$$

Using the localising assumption $x(t^n) = x^n$, we can compute the local truncation error

$$\begin{aligned} T_{n+1} &= x(t^{n+1}) - x^{n+1} \\ \|T_{n+1}\|_2 &= \left\| e^{t^{n+1}(\mathbf{A}+\mathbf{B})} x_0 - e^{k\mathbf{A}} e^{k\mathbf{B}} x^n \right\|_2 \\ &= \left\| e^{(t^n+k)(\mathbf{A}+\mathbf{B})} x_0 - e^{k\mathbf{A}} e^{k\mathbf{B}} x^n \right\|_2. \end{aligned}$$

Now, because the operator $(\mathbf{A} + \mathbf{B})$ commutes with itself, we can split the exponential.

$$\begin{aligned} \|T_{n+1}\|_2 &= \left\| e^{k(\mathbf{A}+\mathbf{B})} e^{t^n(\mathbf{A}+\mathbf{B})} x_0 - e^{k\mathbf{A}} e^{k\mathbf{B}} x^n \right\|_2 \\ &= \left\| \left(e^{k(\mathbf{A}+\mathbf{B})} - e^{k\mathbf{A}} e^{k\mathbf{B}} \right) x^n \right\|_2. \end{aligned}$$

Substituting the series definition of the exponential, we see that

$$\|T_{n+1}\|_2 = \left\| \left[\sum_{j=1}^{\infty} \frac{[k(\mathbf{A}+\mathbf{B})]^j}{j!} - \left(\sum_{m=1}^{\infty} \frac{(k\mathbf{A})^m}{m!} \right) \left(\sum_{n=1}^{\infty} \frac{(k\mathbf{B})^n}{n!} \right) \right] x^n \right\|_2. \quad (3.9)$$

We can use the triangle inequality,

$$\begin{aligned} \|T_{n+1}\|_2 &\leq \left\| x^n + k(\mathbf{A} + \mathbf{B})x^n + \frac{k^2}{2}(\mathbf{A} + \mathbf{B})^2x^n + \frac{k^3}{6}(\mathbf{A} + \mathbf{B})^3x^n \right. \\ &\quad \left. - \left(\mathbf{I} + k\mathbf{A} + \frac{k^2}{2}\mathbf{A}^2 + \frac{k^3}{6}\mathbf{A}^3 \right) \left(\mathbf{I} + k\mathbf{B} + \frac{k^2}{2}\mathbf{B}^2 + \frac{k^3}{6}\mathbf{B}^3 \right) x^n \right\|_2 + \mathcal{O}(k^4), \end{aligned}$$

and group like terms

$$\begin{aligned} \|T_{n+1}\|_2 &\leq k^2 \left\| \frac{1}{2}(\mathbf{A} + \mathbf{B})^2x^n - \left(\frac{1}{2}\mathbf{A}^2 + \mathbf{AB} + \frac{1}{2}\mathbf{B}^2 \right)x^n \right\|_2 + \mathcal{O}(k^3) \\ &= k^2 \|[\mathbf{B}, \mathbf{A}]x^n\|_2 + \mathcal{O}(k^3) \\ &= \mathcal{O}(k^2), \end{aligned} \tag{3.10}$$

for $[\mathbf{B}, \mathbf{A}] = \mathbf{BA} - \mathbf{AB}$ the commutator of \mathbf{B} and \mathbf{A} . Since the local error is of order 2, this means that the Lie splitting method is of order $2 - 1 = 1$.

3.3 Strang splitting method

The Strang splitting method is another treatment of problem (3.8), with $P = 3$, $\mathbf{C}_1 = \frac{1}{2}\mathbf{A}$, $\mathbf{C}_2 = \mathbf{B}$, and $\mathbf{C}_3 = \frac{1}{2}\mathbf{A}$.

By applying Lemma 3.2, we can obtain the Strang local approximation

$$x^{n+1} = e^{\frac{1}{2}k\mathbf{A}}e^{k\mathbf{B}}e^{\frac{1}{2}k\mathbf{A}}x^n.$$

Furthermore, we can get an analogue of (3.9) for the Strang method

$$\begin{aligned} \|T_{n+1}\|_2 &= \left\| \left[e^{k(\mathbf{A}+\mathbf{B})} - e^{\frac{1}{2}k\mathbf{A}}e^{k\mathbf{B}}e^{\frac{1}{2}k\mathbf{A}} \right] x^n \right\|_2 \\ &= \left\| \sum_{j=1}^{\infty} \frac{[k(\mathbf{A} + \mathbf{B})]^j}{j!} - \left(\sum_{\ell=1}^{\infty} \frac{\left(\frac{1}{2}k\mathbf{A}\right)^{\ell}}{\ell!} \right) \left(\sum_{m=1}^{\infty} \frac{(k\mathbf{B})^m}{m!} \right) \left(\sum_{n=1}^{\infty} \frac{\left(\frac{1}{2}k\mathbf{A}\right)^n}{n!} \right) \right\|_2. \end{aligned}$$

After many lines of expanding brackets, this gives

$$\|T_{n+1}\|_2 \leq \frac{k^3}{6} \left\| \frac{1}{4}\mathbf{A}^2\mathbf{B} - \frac{1}{2}\mathbf{ABA} + \frac{1}{4}\mathbf{BA}^2 - \frac{1}{2}\mathbf{AB}^2 + \mathbf{BAB} - \frac{1}{2}\mathbf{B}^2\mathbf{A} \right\|_2 + \mathcal{O}(k^4).$$

All terms of order 1, k , and k^2 cancel out for all \mathbf{A} and \mathbf{B} . Therefore, we have that $\|T_{n+1}\|_2 = \mathcal{O}(k^3)$, so the Strang splitting method is of order 2.

3.4 Experimental Order of Convergence

In the previous sections, we have seen that, analytically, the Strang method is of order 2, and the Lie method is of order 1. It is reassuring to check this computationally, which is what this short section will deal with.

Let r be the order of some numerical method. Let T, t^n and k be defined as above, so that $T = t^N = Nk$. Then, we assume that there exists some constant c independent of k such that

$$\|x^N - x(t^N)\|_2 \approx ck^r. \quad (3.11)$$

In other words, $\|x^N - x(T)\|_2 = \mathcal{O}(k^r)$.

Now, consider performing the same numerical scheme, but with a time-step $\frac{k}{2}$. Let $\tilde{t}^n = \frac{nk}{2}$ be the time points for this experiment, with \tilde{x}^n being the approximation of $x(\tilde{t}^n)$. We again have that, for $k \rightarrow 0$,

$$\|\tilde{x}^{2N} - x(T)\|_2 \approx c \left(\frac{k}{2}\right)^r \quad (3.12)$$

for the *same* constant c .

Therefore, by combining (3.11) and (3.12) and rearranging using logarithm rules, we obtain the Experimental Order of Convergence (EOC) r :

$$r = \log_2 (\|x(T) - x^N\|_2) - \log_2 (\|x(T) - \tilde{x}^{2N}\|_2).$$

Now, we will take a look at an example in order to confirm the analytical results from the previous sections.

Let

$$\mathbf{A} = \begin{bmatrix} 3 & 0 \\ 0 & -2 \end{bmatrix} \quad \text{and} \quad \mathbf{B} = \begin{bmatrix} 0 & -2 \\ 2 & 0 \end{bmatrix},$$

such that $\mathbf{C} = \mathbf{A} + \mathbf{B} = \begin{bmatrix} 3 & -2 \\ 2 & -2 \end{bmatrix}$, and the ODE we seek to approximate is

$$\left. \begin{aligned} \frac{d\mathbf{x}}{dt} &= \mathbf{Cx}(t) \\ \mathbf{x}(0) &= \mathbf{x}_0 = [1, 1]^T \end{aligned} \right\} t \in [0, T]$$

Therefore, the Lie-splitting scheme is described by the iterative system

$$\left. \begin{aligned} \mathbf{x}^0 &= [1, 1]^T \\ \mathbf{x}^{n+1} &= e^{k\mathbf{A}} e^{k\mathbf{B}} \mathbf{x}^n, \end{aligned} \right\} 0 \leq n < N := \frac{T}{k}$$

$\mathbf{x}(t) = [x_1(t), x_2(t)]^T \in \mathbb{C}^2$, so this is a system of two linear differential equations. Since \mathbf{x} is a discrete vector, the error is defined as

$$\|\mathbf{x}(T) - \mathbf{x}^N\|_{\ell^2} := \frac{1}{2} \sqrt{(x_1(t) - x_1^N)^2 + (x_2(t) - x_2^N)^2}$$

and

$$r = \log_2 (\|\mathbf{x}(T) - \mathbf{x}^N\|_{\ell^2}) - \log_2 (\|\mathbf{x}(T) - \tilde{\mathbf{x}}^{2N}\|_{\ell^2}).$$

We have a final time of $T = 1.2$, and time steps $k_j = \frac{0.1}{2^j}$, $0 \leq j \leq 8$, which go down in powers of two in order to compute the EOC. The table below shows the results to 5 decimal places.

| k | Lie EOC | Strang EOC |
|---------------------|---------|------------|
| 0.1 | — | — |
| 0.1×2^{-1} | 0.91900 | 1.99039 |
| 0.1×2^{-2} | 0.96279 | 1.99758 |
| 0.1×2^{-3} | 0.98231 | 1.99939 |
| 0.1×2^{-4} | 0.99140 | 1.99985 |
| 0.1×2^{-5} | 0.99576 | 1.99996 |
| 0.1×2^{-6} | 0.99790 | 1.99999 |
| 0.1×2^{-7} | 0.99895 | 2.00000 |
| 0.1×2^{-8} | 0.99948 | 2.00000 |

Table 3.1: Experimental order of convergence for Lie and Strang splitting methods applied to a two-dimensional matrix system.

These results were computed using Python, and the code can be found in Appendix B.

This nicely confirms our analytical results! The EOC for the Lie splitting method tends to 1, and the Strang EOC tends to 2, as expected.

Chapter 4

Semi-discretization

In this section, we will look at applying the splitting methods introduced in the previous chapters to the semi-classical Schrödinger equation (2.2) in *time only*. Later, we will use Fourier methods for the discretization in space.

4.1 Operators for the splitting method

Note that the Schrödinger equation (2.2) is equivalent to

$$\frac{\partial u}{\partial t} = i\frac{\varepsilon}{2} \frac{\partial^2 u}{\partial x^2} - \frac{i}{\varepsilon} V(x)u.$$

Now, we define the following operators for our splitting method

$$\begin{aligned}\mathcal{A}^\varepsilon &:= -\frac{i}{\varepsilon} V(x), \\ \mathcal{B}^\varepsilon &:= i\frac{\varepsilon}{2} \frac{\partial^2}{\partial x^2}.\end{aligned}\tag{4.1}$$

The intuition behind this choice of \mathcal{A} and \mathcal{B} is that the operators act on very different scales - $\mathcal{A}^\varepsilon = \mathcal{O}(\frac{1}{\varepsilon})$, while $\mathcal{B}^\varepsilon = \mathcal{O}(\varepsilon)$. Furthermore, \mathcal{B} generates a PDE similar to the heat equation, while \mathcal{A} generates a first-order IVP, both of which are relatively simple to solve independently.

These then give rise to the following sub-problems:

$$\left. \begin{array}{l} \frac{\partial v}{\partial t} = \mathcal{A}^\varepsilon v = -\frac{i}{\varepsilon} V(x)v \\ v(a, t) = w(b, t) \\ v_x(a, t) = v_x(b, t) \\ v(x, t = \tau) = v_0(x) \end{array} \right\} t > \tau, x \in [a, b].\tag{4.2}$$

and

$$\left. \begin{array}{l} \frac{\partial w}{\partial t} = \mathcal{B}^\varepsilon w = i \frac{\varepsilon}{2} \frac{\partial^2 w}{\partial x^2} \\ w(a, t) = w(b, t) \\ w_x(a, t) = w_x(b, t) \\ w(x, t = \tau) = w_0(x) \end{array} \right\} t > \tau, x \in [a, b], \quad (4.3)$$

Lemma 4.1. *For a solution $v(x, t)$ of (4.2),*

$$\|v(t)\|_{L^2} = \|v_0\|_{L^2} \quad \forall t \geq \tau.$$

Proof. Taking real parts of the inner product with v ,

$$\operatorname{Re} \left(\int_a^b \frac{\partial v}{\partial t} \bar{v} dx \right) = \operatorname{Re} \left(-i \frac{\varepsilon}{2} \int_a^b V(x) |v|^2 dx \right).$$

The integrand on the right hand side is always real, so the entire right hand side is the real part of a purely imaginary quantity. Applying Lemma 2.1 to the left hand side, we get

$$\frac{d}{dt} \|w(t)\|_{L^2}^2 = 0$$

and so $\|w(t)\|_{L^2} = \|w_0\|_{L^2}$, as required. \square

Lemma 4.2. *For a solution $w(x, t)$ of (4.3),*

$$\|w(t)\|_{L^2} = \|w_0\|_{L^2} \quad \forall t \geq \tau.$$

Proof. Taking real parts of the inner product $\langle \cdot, w \rangle$ on both sides,

$$\operatorname{Re} \left(\int_a^b \frac{\partial w}{\partial t} \bar{w} dx \right) = \operatorname{Re} \left(\int_a^b i \frac{\varepsilon}{2} \frac{\partial^2 w}{\partial x^2} \bar{w} dx \right).$$

By Lemmas 2.1 and 2.2 on the left and right hand side respectively,

$$\begin{aligned} \frac{\varepsilon}{2} \frac{d}{dt} \|w(t)\|_{L^2}^2 &= \operatorname{Re} \left(-i \frac{\varepsilon}{2} \left\| \frac{dw}{dx} \right\|_{L^2}^2 \right) \\ \frac{d}{dt} \|w(t)\|_{L^2} &= 0 \\ \|w(t)\|_{L^2} &= \|w_0\|_{L^2} \quad \forall t \geq \tau. \end{aligned}$$

\square

4.2 The Lie splitting method in the semi-discrete case

Let $0 =: t^0 < t^1 < \dots < t^N := T$ be a partition of $[0, T]$ and let $k = t^{n+1} - t^n, 0 \leq n \leq N - 1$ be the constant time step.

The semi-discrete case consists of only discretizing (2.2) in time (keeping the spatial variable continuous). This reduces the numerical side of the problem to only an initial-value-problem, since the boundary conditions apply only to the spatial variable.

Therefore, recalling (4.1), the equivalent to (3.8) applied to the Schrödinger equation is

$$\left. \begin{aligned} \frac{\partial u}{\partial t} &= (\mathcal{A}^\varepsilon + \mathcal{B}^\varepsilon)u(x, t) \\ u(x, t = 0) &= u_0(x) \end{aligned} \right\} t > 0, x \in [a, b].$$

From time $t = t^n$ to $t = t^{n+1}$, the Schrödinger equation (2.2) is solved in two steps.

First, we solve

$$\frac{\partial u}{\partial t} = \mathcal{A}^\varepsilon u(x, t) \quad (4.4)$$

for one time step, followed by solving

$$\frac{\partial u}{\partial t} = \mathcal{B}^\varepsilon u(x, t) \quad (4.5)$$

for the same time step.

Lemma 4.3.

$$U^{n+1}(x) = e^{k\mathcal{B}^\varepsilon} e^{k\mathcal{A}^\varepsilon} U^n(x), \quad t \in (t^n, t^{n+1}]$$

for $U^n(x)$ the approximation of $u(x, t = t^n)$ yielded by the Lie splitting method applied to the Schrödinger equation (2.2).

Proof. Recalling (3.8), we first solve

$$\left. \begin{aligned} \frac{\partial U^*}{\partial t} &= -i \frac{V(x)}{\varepsilon} U(x, t) = \mathcal{A}^\varepsilon U^*(x, t) \\ U^*(x, t = t^n) &= U^n(x) \end{aligned} \right\} t \in (t^n, t^{n+1}], x \in [a, b]. \quad (4.6)$$

Using Lemma 3.1, we have that

$$U^*(x, t) = e^{(t-t^n)\mathcal{A}^\varepsilon} U^n(x), \quad t \in (t^n, t^{n+1}]. \quad (4.7)$$

We then solve

$$\left. \begin{aligned} \frac{\partial U}{\partial t} &= i \frac{\varepsilon}{2} \frac{\partial^2 U^*}{\partial x^2} = \mathcal{B}^\varepsilon U(x, t) \\ U(x, t = t^n) &= U^*(x, t^{n+1}) \end{aligned} \right\} t \in (t^n, t^{n+1}], x \in [a, b],$$

so,

$$U(x, t) = e^{(t-t^n)\mathcal{B}^\varepsilon} U^*(x, t^{n+1}). \quad (4.8)$$

Now, by substituting (4.7) into (4.8),

$$\begin{aligned} U^{n+1} &= U(x, t = t^{n+1}) \\ &= e^{k\mathcal{B}^\varepsilon} e^{k\mathcal{A}^\varepsilon} U^n(x), \quad t \in (t^n, t^{n+1}]. \end{aligned}$$

□

Remark 4.1. It is important to note that, in the semi-discrete case, we assume that we have an exact expression for $e^{i\frac{\varepsilon}{2}\frac{\partial^2}{\partial x^2}}$. This operator will be approximated in the fully discrete case.

Lemma 4.4. The Lie splitting method is unconditionally stable. For any time step k ,

$$\|U^n\|_{L^2} = \|U^0\|_{L^2}, \quad 0 \leq n \leq N$$

Proof. This is most easily proved by induction. The base case is trivial: $\|U^0\|_{L^2} = \|U^0\|_{L^2}$.

Now note that, to obtain U^{n+1} from U^n , we first solve (4.6). Using Lemma 4.1, we have that

$$\|U^*\|_{L^2} = \|U^n\|_{L^2}$$

Then, using Lemma 4.2, we have that

$$\|U^{n+1}\|_{L^2} = \|U^*\|_{L^2},$$

so,

$$\|U^{n+1}\|_{L^2} = \|U^n\|_{L^2}.$$

Now suppose that

$$\|U^n\|_{L^2} = \|U^0\|_{L^2}.$$

We then have that $\|U^{n+1}\|_{L^2} = \|U^0\|_{L^2}$, completing the proof.

□

4.3 Lie splitting error for time-independent potentials

First, we define some notation and assumptions.

The L^∞ -norm of a continuous and bounded function v in (a, b) is denoted by $\|\cdot\|_{L^\infty}$ and it is defined as

$$\|v\|_{L^\infty} = \sup_{x \in (a, b)} |v(x)|.$$

To investigate the dependence of the small parameter ε (Planck's constant) with respect to the time-step and the spatial mesh-size of the time-splitting spectral schemes we will be considering later, we assume from now on that the data of the problem satisfy some additional properties.

In particular, suppose u is a solution of (2.2) with initial condition $u(x, t = 0) = u_0(x)$. Then, we assume that for all non-negative integers s , there exist positive constants A_s, B_s , independent of the Planck constant ε such that

$$(A1) \quad \left\| \frac{d^s u_0}{dx^s} \right\|_{L^2} \leq \frac{A_s}{\varepsilon^s},$$

$$(A2) \quad \left\| \frac{d^s V}{dx^s} \right\|_{L^\infty} \leq B_s.$$

Furthermore, given these assumptions, it is possible to show (but we will assume, as is done in [BJM02]) that for all nonnegative integers s_1, s_2 , there exists a positive constant E_i , independent of ε such that

$$(A3) \quad \max_{0 \leq t \leq T} \left\| \frac{\partial^{s_1+s_2}}{\partial t^{s_1} \partial x^{s_2}} u(x, t) \right\|_{L^2} \leq \frac{E_{s_1+s_2}}{\varepsilon^{s_1+s_2}}.$$

For example, Assumption (A1) is satisfied if the initial data u_0 is of Wentzel-Kramers-Brillouin (WKB) form

$$u_0(x) = \sqrt{n_0(x)} e^{iS_0(x)/\varepsilon}, \quad x \in \mathbb{R},$$

since each higher derivative in x will bring down a factor of $\frac{1}{\varepsilon}$ from the exponent.

We will use this type of initial data throughout this work, with $n_0, S_0 \in C^\infty$, $(b-a)$ -periodic, and n_0 strictly non-negative with $\lim_{|x| \rightarrow \infty} n_0(x) = 0$. The final property must be true of all probability density functions in order to satisfy the honesty condition.

Lemma 4.5. *Let $u = u(x, t)$ be an exact solution of (2.2), $U^n = U^n(x)$ be the discrete approximation of u at $t = t^n$ given by the Lie splitting method, and T_{n+1} be the local truncation error. Under assumptions (A1) and (A2),*

$$\|T_{n+1}\|_{L^2} = \mathcal{O}\left(\frac{k^2}{\varepsilon}\right)$$

Proof. For the local error, we take the localising assumption $U^n(x) = u(x, t = t^n)$, $\forall x \in [a, b]$. Also note that U^n is a univariate function, and therefore $\frac{\partial^n U^n}{\partial x^n} = \frac{d^n U^n}{dx^n}$.

Using (3.10), we have

$$\begin{aligned} \|T_{n+1}\|_{L^2} &= \left\| \frac{k^2}{2} (\mathcal{B}\mathcal{A} - \mathcal{A}\mathcal{B}) U^n + \mathcal{O}(k^3) \right\|_{L^2} \\ &\leq \frac{k^2}{2} \left\| \frac{1}{2} \frac{d^2}{dx^2} (V(x) U^n) - \frac{1}{2} V(x) \frac{d^2 U^n}{dx^2} \right\|_{L^2} + \mathcal{O}(k^3) \\ &= \frac{k^2}{2} \left\| \frac{dV}{dx} \frac{dU^n}{dx} + \frac{1}{2} \frac{d^2 V}{dx^2} U^n \right\|_{L^2} + \mathcal{O}(k^3) \\ &\leq \frac{k^2}{2} \left(\left\| \frac{dV}{dx} \frac{dU^n}{dx} \right\|_{L^2} + \frac{1}{2} \left\| \frac{d^2 V}{dx^2} U^n \right\|_{L^2} \right) + \mathcal{O}(k^3). \end{aligned}$$

Noticing the two terms of the form $\left\| \frac{d^s V}{dx^s} \frac{d^r U^n}{dx^r} \right\|_{L^2}$, we first have that

$$\begin{aligned} \left\| \frac{d^s V}{dx^s} \frac{d^r U^n}{dx^r} \right\|_{L^2} &= \sqrt{\int_a^b \left(\frac{d^s V}{dx^s} \right)^2 \left(\frac{d^r U^n}{dx^r} \right)^2 dx} \\ &\leq \left(\sup_{x \in (a,b)} \frac{d^s V}{dx^s} \right) \sqrt{\int_a^b \left(\frac{d^r U^n}{dx^r} \right)^2 dx} \\ &= \left\| \frac{d^s V}{dx^s} \right\|_{L^\infty} \left\| \frac{d^r U^n}{dx^r} \right\|_{L^2} \leq B_s \frac{E_r}{\varepsilon^r}. \end{aligned}$$

Thus, we obtain

$$\begin{aligned} \|T_{n+1}\|_{L^2} &\leq \frac{k^2}{2} \left(B_1 \frac{E_1}{\varepsilon} + \frac{1}{2} B_2 E_0 \right) + \mathcal{O}(k^3) \\ &= \mathcal{O}\left(\frac{k^2}{\varepsilon}\right). \end{aligned}$$

Since

$$0 \leq \|T_{n+1}\|_{L^2} \leq \mathcal{O}\left(\frac{k^2}{\varepsilon}\right),$$

the statement of the lemma then follows. □

Remark 4.2. The global truncation error for the Lie splitting method is $\mathcal{O}\left(\frac{k}{\varepsilon}\right)$, which suggests that we should choose $k = \mathcal{O}(\varepsilon)$ in order to expect convergence.

4.4 The Strang splitting method in the semi-discrete case

The Strang splitting method can easily be obtained from the previous chapters.

$$U^{n+1}(x) = e^{\frac{1}{2}k\mathcal{A}^\varepsilon} e^{k\mathcal{B}^\varepsilon} e^{\frac{1}{2}k\mathcal{A}^\varepsilon} U^n(x), \quad t \in (t^n, t^{n+1}] \quad (4.9)$$

Lemma 4.6. Let $u = u(x, t)$ be an exact solution of (2.2), $U^n = U^n(x)$ be the discrete approximation of u at $t = t^n$ given by the Strang splitting method (4.9), and T_{n+1} be the local truncation error. Under assumption (A1),

$$\|T_{n+1}\|_{L^2} = \mathcal{O}\left(\frac{k^3}{\varepsilon}\right)$$

Proof. This proof follows many of the same steps as Lemma 4.5. We have that

$$\begin{aligned}\|T_{n+1}\|_{L^2} &= \left\| \left(e^{\frac{1}{2}k\mathcal{A}} e^{k\mathcal{B}} e^{\frac{1}{2}k\mathcal{A}} - e^{k(\mathcal{A}+\mathcal{B})} \right) U^n \right\|_{L^2} \\ &\leq \frac{k^3}{6} \left\| \left(\frac{1}{4}\mathcal{A}^2\mathcal{B} - \frac{1}{2}\mathcal{A}\mathcal{B}\mathcal{A} + \frac{1}{4}\mathcal{B}\mathcal{A}^2 - \frac{1}{2}\mathcal{B}^2\mathcal{A} - \frac{1}{2}\mathcal{A}\mathcal{B}^2 + \mathcal{B}\mathcal{A}\mathcal{B} \right) U^n \right\|_{L^2} + \mathcal{O}(k^4) \\ &= \frac{k^3}{6} \left\| \frac{i\varepsilon}{4} \frac{d^2V}{dx^2} \frac{d^2U^n}{dx^2} - \frac{i}{4\varepsilon} \frac{d^2}{dx^2} (V(x)^2) + \frac{i}{2\varepsilon} V(x) U^n(x, t) \frac{d^2V}{dx^2} \right\|_{L^2} + \mathcal{O}(k^4).\end{aligned}$$

Now, applying the triangle inequality to each term as in the proof for Lemma 4.5, we arrive at the statement of Lemma 4.6 \square

Both splitting errors are non-zero due to the fact that \mathcal{A}^ε and \mathcal{B}^ε do not commute. In the case where $V(x) \equiv V$ is a constant potential, then we can pull V through the derivative in \mathcal{A}^ε , so the local and global errors are then zero.

Chapter 5

Spectral approximation

So far, we have discretised the linear Schrödinger equation in time only using the two aforementioned splitting methods. In order to implement these methods computationally, we need to take into account the spatial domain of the problem.

Numerically, (4.4) is explicitly and exactly solvable for V independent of t , since the solution is

$$u(x, t) = e^{tV(x)} u_0(x),$$

which holds true for any initial condition u_0 . However, the solution to (4.5), i.e. the heat equation, is not as trivial. Analytically solving the problem for periodic boundary conditions gives an infinite Fourier series solution, which is not computationally exact. This motivates the use of truncated Fourier series to approximate the solution to (4.5) using spectral methods.

5.1 Fourier method

Let $h = \Delta x > 0$ be the spatial mesh size with $h = \frac{b-a}{M}$ for M an *even* positive integer, and let the spatial grid points be

$$x_j := a + jh, \quad 0 \leq j \leq M.$$

An even number of grid points is used because odd and even M need to be treated slightly differently. Let also $\mu_\ell = \frac{2\pi\ell}{b-a}$ and consider the finite-dimensional subspace \mathbb{V}_M of $L^2(a, b)$

$$\mathbb{V}_M := \text{span} \left\{ e^{i\mu_\ell(x-a)} \mid -\frac{M}{2} \leq \ell \leq \frac{M}{2} - 1 \right\}.$$

For a $(b-a)$ -periodic function f we denote by f_I its *trigonometric interpolant* on the grid $\{x_0, x_1, \dots, x_{M-1}\}$

$$f_I = \frac{1}{M} \sum_{\ell=-\frac{M}{2}}^{\frac{M}{2}-1} \hat{f}_\ell e^{i\mu_\ell(x-a)}, \quad \text{with} \quad \hat{f}_\ell = \sum_{j=0}^{M-1} f(x_j) e^{-i\mu_\ell(x_j-a)}.$$

The coefficients \hat{f}_ℓ are called the *discrete Fourier coefficients* of f , and are chosen so that $f_I(x_j) = f(x_j)$. f_I is both the truncated Fourier series of f , and the projection of f onto \mathbb{V}_M . When f is periodic and smooth, we have that

$$\lim_{M \rightarrow \infty} f_I = f$$

pointwise. If f is not smooth and periodic, then the Gibbs phenomenon can occur at discontinuities. In this case, the limit above is true in the ℓ^2 -norm, but not pointwise.

So, applying this to $\frac{\partial u}{\partial t} - i\frac{\varepsilon}{2} \frac{\partial^2 u}{\partial x^2} = 0$, we assume that we have at our disposal the approximations U_j^n of $u(x_j, t^n)$, $0 \leq j \leq M-1$. Let

$$U_I^n = \frac{1}{M} \sum_{\ell=-\frac{M}{2}}^{\frac{M}{2}-1} \hat{U}_\ell^n e^{i\mu_\ell(x-a)}, \quad \text{and} \quad \hat{U}_\ell^n = \sum_{j=0}^{M-1} U_j^n e^{-i\mu_\ell(x_j-a)}.$$

In a numerical context, the x values will be bound to the x_j knots defined above. Due to the defining property of an interpolant, if we construct the interpolant on these knots, we will also have that $U_I^n(x_j) = U^n(x_j)$.

This interpolant is particularly useful when calculating the derivative. Note that

$$\frac{d}{dx} U_I^n(x) = \frac{1}{M} \sum_{\ell=-\frac{M}{2}}^{\frac{M}{2}-1} i\mu_\ell \hat{U}_\ell^n e^{i\mu_\ell(x-a)}.$$

Therefore, to approximate the derivative of U^n at $x = x_j$ we can perform the following steps:

$$U_j^n \xrightarrow{\text{DFT}} \hat{U}_\ell^n \xrightarrow{\frac{d^2}{dx^2}} -\mu_\ell^2 \hat{U}_\ell^n \xrightarrow{\text{DFT}^{-1}} \frac{dU^n}{dx}(x_j),$$

where the DFT is the discrete Fourier transform, sending $\{U_0^n, \dots, U_M^n\}$ to $\left\{ \hat{U}_{-\frac{M}{2}}^n, \dots, \hat{U}_{\frac{M}{2}-1}^n \right\}$.

Note that this is an approximation because $U_I^n(x) \neq U(x, t^n)$ in between knots x_j .

It can be shown that this method of differentiation is a generalization of the finite difference method for a maximally sized stencil. See [Luc24] for a more detailed exploration of the topic.

5.2 Lie splitting spectral method

The Lie splitting spectral method for the Schrödinger equation (2.2) can be described as follows.

Solve exactly the problem

$$\left. \begin{aligned} \frac{\partial U^*}{\partial t} + \frac{i}{\varepsilon} V(x) &= 0 \\ U^*(x, t^n) &= U^n(x, t^n) \end{aligned} \right\} t \in (t^n, t^{n+1}], \quad (5.1)$$

followed by solving on the finite-dimensional space \mathbb{V}_M the problem

$$\left. \begin{aligned} & \frac{\partial U}{\partial t} - i\frac{\varepsilon}{2} \frac{\partial^2 U}{\partial x^2} = 0 \\ & U(x, t^n) = U^*(x, t^{n+1}) \end{aligned} \right\} t \in (t^n, t^{n+1}]. \quad (5.2)$$

Then, the approximation at $t = t^{n+1}$ is $U^{n+1}(x) = U(x, t^{n+1})$ and, for $0 \leq j \leq M-1$, the approximations U_j^{n+1} of $u(x_j, t^{n+1})$ are given by $U_j^{n+1} := U^{n+1}(x_j)$. It is important to once again note that the periodic boundary conditions are included in the choice of basis functions for \mathbb{V}_M .

Solving (5.1) exactly gives

$$U^*(x, t) = e^{-\frac{i}{\varepsilon} V(x)(t-t^n)} U^n(x, t^n),$$

which has the trigonometric interpolant

$$U_I^*(x, t) = \frac{1}{M} \sum_{\ell=-\frac{M}{2}}^{\frac{M}{2}-1} \hat{U}_\ell^*(t) e^{i\mu_\ell(x-a)}.$$

Now, let

$$U_I(x, t) = \frac{1}{M} \sum_{\ell=-\frac{M}{2}}^{\frac{M}{2}-1} \hat{U}_\ell(t) e^{i\mu_\ell(x-a)} \quad (5.3)$$

be the trigonometric interpolant of the solution to (5.2).

Then, substituting trigonometric interpolants in place of exact solutions, we get the following version of (5.2).

$$\left. \begin{aligned} & \frac{1}{M} \sum_{\ell=-\frac{M}{2}}^{\frac{M}{2}-1} \left(\frac{\partial \hat{U}_\ell}{\partial t} + \frac{i\mu_\ell^2 \varepsilon}{2} \hat{U}_\ell \right) e^{i\mu_\ell(x-a)} = 0 \\ & \hat{U}_\ell(t^n) = \hat{U}_\ell^*(t^{n+1}) \end{aligned} \right\} t \in (t^n, t^{n+1}] \quad (5.4)$$

Given that the standard basis $\left\{ e^{i\mu_\ell(x-a)} \mid -\frac{M}{2} \leq \ell \leq \frac{M}{2} - 1 \right\}$ for \mathbb{V}_M is linearly independent, we readily obtain that (5.4) is now equivalent to solving the M equations

$$\left. \begin{aligned} & \frac{\partial \hat{U}_\ell}{\partial t} + \frac{i\mu_\ell^2 \varepsilon}{2} \hat{U}_\ell \\ & \hat{U}_\ell(t^n) = \hat{U}_\ell^*(t^{n+1}) \end{aligned} \right\} -\frac{M}{2} \leq \ell \leq \frac{M}{2} - 1. \quad (5.5)$$

Finally, combining (5.5), (5.2), (5.3), and performing the procedure detailed above, the Lie splitting spectral approximations for problem (2.2) can be concisely given by:

For $0 \leq n \leq N-1$ and $0 \leq j \leq M-1$,

$$\left. \begin{aligned} U_j^* &= e^{-k \frac{i}{\varepsilon} V(x)} U_j^n \\ U_j &= \frac{1}{M} \sum_{\ell=-\frac{M}{2}}^{\frac{M}{2}-1} e^{-\frac{i\varepsilon\mu_\ell^2}{2} k} e^{i\mu_\ell(x_j-a)} \hat{U}_\ell^n \end{aligned} \right\} \quad (5.6)$$

with

$$\hat{U}_\ell^n = \sum_{j=0}^{M-1} U_j^n e^{-i\mu_\ell(x_j-a)}$$

the *discrete Fourier coefficients* of U^n , and

$$U_j^0 = u_0(x_j).$$

While we have proven conservation of total mass density for the Lie splitting method in Section 4.3, we assumed exact solutions to both subproblems. Since we are using a non-exact Fourier method to solve the diffusive part of the problem, some further analysis is necessary.

Theorem 5.1 (Lie splitting spectral stability). *Let \mathbf{U}^n be the discrete Lie splitting spectral approximation, numerically integrated from an initial condition vector \mathbf{U}^0 .*

Then, we have that

$$\|\mathbf{U}^n\|_{\ell^2} = \|\mathbf{U}^0\|_{\ell^2} \quad \forall n \in \mathbb{Z}^{\geq 0},$$

i.e. the Lie splitting spectral method is unconditionally stable for all spatial mesh sizings and time steps.

Proof. We will again prove this by induction on n , in a similar fashion to Lemma 4.4. The base case for $n = 0$ is obvious.

For the Lie splitting spectral method outlined in (5.6), we have

$$\begin{aligned} \|\mathbf{U}^{n+1}\|_{\ell^2}^2 &= \frac{1}{M} \sum_{j=1}^M |U_j^{n+1}|^2 = \frac{1}{M} \sum_{j=1}^M \left| e^{-\frac{ik}{\varepsilon} V(x_j)} U_j^* \right|^2 = \frac{1}{M} \sum_{j=1}^M |U_j^*|^2 \\ &= \frac{1}{M} \sum_{j=1}^M \left| \frac{1}{M} \sum_{\ell=-\frac{M}{2}}^{\frac{M}{2}-1} e^{-\frac{i\varepsilon\mu_\ell^2}{2} k} e^{i\mu_\ell(x_j-a)} \hat{U}_\ell^n \right|^2 \\ &= \frac{1}{M} \sum_{j=1}^M \left[\frac{1}{M^2} \left(\sum_{\ell=-\frac{M}{2}}^{\frac{M}{2}-1} \sum_{m=-\frac{M}{2}}^{\frac{M}{2}-1} e^{-\frac{i\varepsilon\mu_\ell^2}{2} k} e^{i\mu_\ell(x_j-a)} e^{\frac{i\varepsilon\mu_m^2}{2} k} e^{-i\mu_m(x_j-a)} \hat{U}_\ell^n \overline{\hat{U}_m^n} \right) \right] \\ &= \frac{1}{M^3} \sum_{j=1}^M \sum_{\ell=-\frac{M}{2}}^{\frac{M}{2}-1} \sum_{m=-\frac{M}{2}}^{\frac{M}{2}-1} e^{-\frac{i\varepsilon k}{2} (\mu_\ell^2 - \mu_m^2)} e^{i(\mu_\ell - \mu_m)(x_j-a)} \hat{U}_\ell^n \overline{\hat{U}_m^n} \\ &= \frac{1}{M^3} \sum_{\ell=-\frac{M}{2}}^{\frac{M}{2}-1} \sum_{m=-\frac{M}{2}}^{\frac{M}{2}-1} e^{-\frac{i\varepsilon k}{2} (\mu_\ell^2 - \mu_m^2) - ia(\mu_\ell - \mu_m)} \hat{U}_\ell^n \overline{\hat{U}_m^n} \sum_{j=1}^M e^{i(\mu_\ell - \mu_m)x_j}. \end{aligned}$$

By the definition of $\mu_\ell = \frac{2\pi\ell}{b-a}$, we have that

$$\sum_{j=1}^M e^{i(\mu_\ell - \mu_m)x_j} = M\delta_{\ell m} = \begin{cases} M & \text{if } \ell = m \\ 0 & \text{if } \ell \neq m \end{cases}$$

thus,

$$\begin{aligned} \|\mathbf{U}^{n+1}\|_{\ell^2}^2 &= \frac{1}{M^3} \sum_{\ell=-\frac{M}{2}}^{\frac{M}{2}-1} M \left| \hat{U}_\ell^n \right|^2 \\ &= \frac{1}{M^2} \sum_{\ell=-\frac{M}{2}}^{\frac{M}{2}-1} \left| \sum_{j=0}^{M-1} U_j^n e^{-i\mu_\ell(x_j-a)} \right|^2 \end{aligned}$$

which, by similar orthogonality arguments as above, simplifies to

$$= \frac{1}{M} \sum_{j=0}^{M-1} |U_j^n|^2 = \|\mathbf{U}^n\|_{\ell^2}^2.$$

Therefore, by the fact that norms are non-negative, we have that

$$\|\mathbf{U}^{n+1}\|_{\ell^2} = \|\mathbf{U}^n\|_{\ell^2}$$

and so, by induction, we obtain the statement of the theorem. \square

Theorem 4.1 in [BJM02] states the following convergence result for the Lie splitting method.

Theorem 5.2. *Let $u = u(x, t)$ be the exact solution of the semi-classical Schrödinger equation (2.2), $\mathbf{U}^N = [U_0^N, \dots, U_M^N]$ be the discrete approximation given by the Lie time-splitting spectral method (5.6) at $t = t^N := T$, and $\mathbf{U}_I^N(x)$ be the trigonometric interpolant of \mathbf{U}^N . Then, assuming $\frac{k}{\varepsilon} = \mathcal{O}(1)$, $\frac{h}{\varepsilon} = \mathcal{O}(1)$, we have for all positive integers $M \geq 1$ that*

$$\|u(T) - \mathbf{U}^N\|_{L^2} \leq G_M \frac{T}{k} \left(\frac{h}{\varepsilon(b-a)} \right)^M + \frac{CTk}{\varepsilon},$$

where C is independent of ε, h, k and M , and G_M is independent of ε, h and k .

Note that this quantity is not the local truncation error, but the global error. The first term, which is exponential in M , is the error from the spectral approximation in space. The second term is the global error resulting from the splitting method in time. By (3.10), the local error is $\mathcal{O}\left(\frac{k^2}{\varepsilon}\right)$. Since the local error accumulates over N steps, the global error is therefore $\mathcal{O}\left(\frac{Nk \times k}{\varepsilon}\right) = \mathcal{O}\left(\frac{Tk}{\varepsilon}\right)$.

This estimate for the Lie splitting spectral error suggests a “meshing strategy”. In other words, for a desired error δ such that

$$\|u(T) - \mathbf{U}^N\|_{L^2} \leq \delta,$$

we should then set our spatial mesh size h and time step k according to

$$\frac{k}{\varepsilon} = \mathcal{O}\left(\frac{\delta}{T}\right), \quad \frac{h}{\varepsilon} = \mathcal{O}\left(\left[\frac{\delta k}{G_m T}\right]^{\frac{1}{M}}\right).$$

Due to the relationship $M \propto \frac{1}{h}$, we can summarise this as, for constant δ ,

$$h = \mathcal{O}(\varepsilon), \quad k = o(\varepsilon).$$

I.e. k must be of lower order than ε . This meshing strategy is based off of L^2 convergence to the wave function u . However, in physical contexts, the wave function is not the quantity of interest - it is the observables, such as position and current density. Using Wigner function analysis and computational experimentation, the authors of [BJM02] have shown that the significantly less restrictive time stepping strategy

$$k = \mathcal{O}(\delta) \tag{5.7}$$

is sufficient for accurate observables. This is a major result - the time step does not need to scale with ε , even for very small ε . This meshing strategy is shown to be effective in Examples 1-3 in Section 6.1.

5.3 Strang splitting spectral method

The Strang splitting spectral method for the semi-classical Schrödinger equation (2.2) can be defined similarly following the description of the semi-discrete Strang splitting method (4.9).

For $0 \leq n \leq N - 1$ and $0 \leq j \leq M - 1$,

$$\left. \begin{aligned} U_j^* &= e^{-\frac{ik}{2\varepsilon}V(x_j)}U_j^n \\ U_j^{**} &= \frac{1}{M} \sum_{\ell=-\frac{M}{2}}^{\frac{M}{2}-1} e^{-\frac{i\varepsilon\mu_\ell^2}{2}k} e^{i\mu_\ell(x_j-a)} \hat{U}_\ell^* \\ U_j^{n+1} &= e^{-\frac{ik}{2\varepsilon}V(x_j)}U_j^{**} \end{aligned} \right\} \tag{5.8}$$

with

$$U_j^0 = u_0(x_j).$$

Theorem 5.3 (Strang splitting spectral stability). *Let \mathbf{U}^n be the discrete Strang splitting spectral approximation, numerically integrated from an initial condition vector \mathbf{U}^0 .*

Then, we have that

$$\|\mathbf{U}^n\|_{\ell^2} = \|\mathbf{U}^0\|_{\ell^2} \quad \forall n \in \mathbb{Z}^{\geq 0},$$

i.e. the Strang splitting spectral method is unconditionally stable for all spatial mesh sizings and time steps.

Proof. This proof is omitted for conciseness. It follows almost exactly the same pattern as Theorem 5.1. \square

5.4 Extensions to d dimensions

Both methods defined in the previous section are applied solely to the one-dimensional Schrödinger equation. We will outline the Strang splitting spectral method for the Schrödinger equation in two spatial dimensions.

The semi-classical Schrödinger equation for a wave function $u(\mathbf{x}, t)$, $\mathbf{x} \in \mathbb{R}^d$ is

$$\frac{\partial u}{\partial t} = i\frac{\varepsilon}{2}\nabla_{\mathbf{x}}^2 u - \frac{i}{\varepsilon}V(\mathbf{x}),$$

for $V : \mathbb{R}^d \rightarrow \mathbb{R}$ the scalar potential function and $\nabla_{\mathbf{x}}^2 = \nabla_{\mathbf{x}} \cdot \nabla_{\mathbf{x}} = \frac{\partial^2}{\partial x_1^2} + \cdots + \frac{\partial^2}{\partial x_d^2}$ the (spatial) Laplacian.

The operators in this case are

$$\begin{aligned}\mathcal{A}^\varepsilon &= -\frac{i}{\varepsilon}V(\mathbf{x}) \\ \mathcal{B}^\varepsilon &= i\frac{\varepsilon}{2}\nabla_{\mathbf{x}}^2.\end{aligned}$$

\mathcal{A}^ε requires no new approach - the solution is still the same, since it is still a first-order constant-coefficient IVP.

However, the approximation of the Laplacian in multiple dimensions takes some more care, since the Fourier method needs to be extended.

From here on, we will assume $d = 2$, however it should be clear how to apply this technique to $d \geq 3$.

The trigonometric interpolant of a function $U(x, y, t)$, $U : \mathbb{R}^2 \times \mathbb{R}^{>0} \rightarrow \mathbb{R}$ is defined as

$$U_I(t) = \frac{1}{MN} \sum_{m=-\frac{M}{2}}^{\frac{M}{2}-1} \sum_{n=-\frac{N}{2}}^{\frac{N}{2}-1} \hat{U}_{m,n}(t) e^{i[\mu_m(x-a_1)+\nu_n(y-a_2)]}$$

for

- Spatial nodes $a_1 =: x_0, \dots, x_M := b_1$ and $a_2 =: y_0, \dots, y_N := b_2$,
- Discrete fourier coefficients $\hat{U}_{m,n}(t)$,
- $\mu_m = \frac{2\pi m}{b_1 - a_1}$, $\nu_n = \frac{2\pi n}{b_2 - a_2}$.

Therefore, we have that

$$\begin{aligned}\nabla_{\mathbf{x}}^2 U_I &= \frac{\partial^2 U_I}{\partial x^2} + \frac{\partial^2 U_I}{\partial y^2} \\ &= \frac{1}{MN} \sum_{m=-\frac{M}{2}}^{\frac{M}{2}-1} \sum_{n=-\frac{N}{2}}^{\frac{N}{2}-1} -(\mu_m^2 + \nu_n^2) \hat{U}_{m,n}(t) e^{i[\mu_m(x-a_1)+\nu_n(y-a_2)]}.\end{aligned}\tag{5.9}$$

Now, let $U_{i,j}^n$ be the approximation of $u(x_i, y_j, t^n)$. Using similar arguments as for the derivation of (5.8), we obtain the following explicit formula for the Strang time-splitting spectral method for the 2-dimensional semi-classical Schrödinger equation.

$$\left. \begin{aligned} U_{i,j}^* &= e^{-\frac{ik}{2\varepsilon} V(x_j, y_j)} U_{i,j}^n \\ U_{i,j}^{**} &= \frac{1}{MN} \sum_{m=-\frac{M}{2}}^{\frac{M}{2}-1} \sum_{n=-\frac{N}{2}}^{\frac{N}{2}-1} -(\mu_m^2 + \nu_n^2) e^{i[\mu_m(x_i-a_1) + \nu_n(y_j-a_2)]} \hat{U}_{m,n}^*(t) \\ U_{i,j}^{n+1} &= e^{-\frac{ik}{2\varepsilon} V(x_i, y_j)} U_{i,j}^{**} \end{aligned} \right\}$$

Chapter 6

Computational results

This section deals with the computational implementation of the time-splitting spectral methods, as well as examines a variety of experiments.

6.1 Numerical Examples

The initial data is bound to the WKB functional form

$$u_0(x) = \sqrt{n_0(x)} e^{iS_0(x)/\varepsilon},$$

with the following conditions:

| Condition | Reason |
|--|--|
| $S_0, n_0 \in C^\infty$ | to satisfy conditions in Chapter 4 |
| $S_0, n_0 : \mathbb{R} \rightarrow \mathbb{R}$ | can be assumed without loss of generality. |
| S_0, n_0 independent of ε | property of WKB form, as well as satisfying (A1) since each application of $\frac{d}{dx}$ will bring down a factor of ε^{-1} . |
| $\lim_{ x \rightarrow \infty} n_0(x) = 0$ | $n(x, t) = u(x, t) ^2$ needs to be a probability density function. |

Note that $|u_0(x)|^2 = n_0(x)$ is the initial position density.

Computationally, the DFT is performed using NumPy's Fast Fourier Transform (fft) algorithm. See Appendix B for the code in Python.

EXAMPLE 1. This is a recreation of Example 1 from [BJM02] with only 3 of the trials. The initial condition is given by

$$n_0(x) = e^{-50(x-0.5)^2} \quad \text{and} \quad S_0(x) = \frac{1}{5} \ln \left(e^{5(x-0.5)} + e^{-5(x-0.5)} \right),$$

And the spatial domain is $x \in [0, 1]$, i.e. $a = 0$ and $b = 1$.

The potential $V(x, t) := 10$ is constant for all x and t . This results in \mathcal{A}^ε and \mathcal{B}^ε commuting. Therefore, $e^{k\mathcal{A}^\varepsilon}$ and $e^{k\mathcal{B}^\varepsilon}$ also commute, and both splitting methods are equivalent and become the

exact-in-time one-step method

$$U_j^N = \underbrace{e^{-\frac{i}{\varepsilon}V_0 T}}_{e^{T\mathcal{B}^\varepsilon}} \underbrace{\frac{1}{M} \sum_{\ell=-\frac{M}{2}}^{\frac{M}{2}-1} e^{-\frac{i\varepsilon\mu_\ell^2}{2}T} e^{i\mu_\ell(x_j-a)} \hat{U}_\ell^0}_{e^{T\mathcal{A}^\varepsilon} U_j^0},$$

where U_j^N is the approximation of $U(x_j, T)$. This method is not exact in space, since we are still using spectral methods to approximate the second derivative.

There is an exact classical limit solution for $\varepsilon \rightarrow 0$ for reference. This limit is derived in Appendix A.2.

The domain is $[0, 1]$, with spatial knots

$$x_j = hj, \quad 0 \leq j \leq M, \quad M = \frac{1}{h}.$$

Plots of the position density and current density observables can be seen in Figure 6.1. We see that for $\frac{h}{\varepsilon} = \frac{625}{256} = \mathcal{O}(1)$, caustics are captured accurately, and the numerical method captures the $\varepsilon \rightarrow 0$ behaviour.

EXAMPLE 2. This is a recreation of Example 3 from [BJM02]. The initial condition is

$$n_0(x) = e^{-50(x-0.5)^2} \quad \text{and} \quad S_0(x) = x + 1,$$

and a potential $V(x) = \frac{x^2}{2}$ for a quantum harmonic oscillator.

The analytical solutions for $\varepsilon \rightarrow 0$ for the observables $n(x, t)$ and $J(x, t)$, obtained from Example 4 in [GM97], are

$$\begin{aligned} n(x, t) &= \frac{1}{|\cos t|} n_0 \left(\frac{x - \sin t}{\cos t} \right), \\ J(x, t) &= \frac{1}{|\cos t|} n_0 \left(\frac{x - \sin t}{\cos t} \right) \frac{1 - x \sin t}{\cos t}. \end{aligned}$$

Plots of the observables are in Figure 6.2. Even for $\varepsilon = 0.04$, the numerical approximation is qualitatively very close to the semi-classical limit. Furthermore, the plots support (5.7) since even for $k = 320\varepsilon$ in row (iii), the solution is captured well.

EXAMPLE 3. This is a recreation of Example 4 from [BJM02]. This is a two-dimensional example with spatial domain $(x, y) \in [-2, 2] \times [-2, 2]$.

The initial condition is

$$n_0(x, y) = e^{-50[(x-0.5)^2 + 0.8(y-0.5)^2]} \quad \text{and} \quad S_0(x, y) = x + \frac{y}{2},$$

with a quadratic potential

$$V(x, y) = \frac{x^2 + y^2}{2}.$$

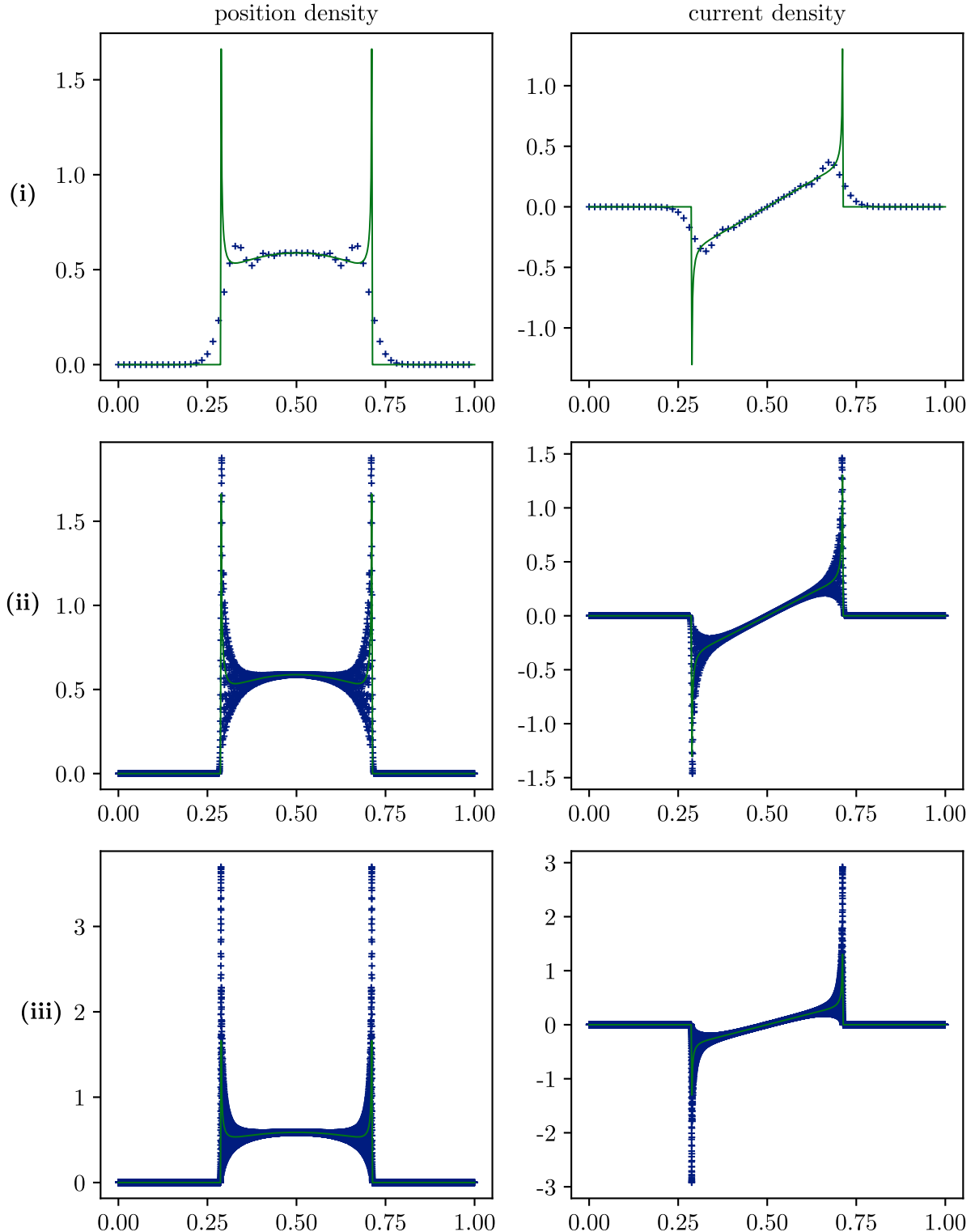


Figure 6.1: Example 1. Numerical solutions at $t = 0.54$ (after caustics form). $V(x) = 10$; $\text{++}+$: numerical solution, — : analytical weak limit; (i) $\varepsilon = 0.0064, h = \frac{1}{64}$; (ii) $\varepsilon = 0.0001, h = \frac{1}{4096}$; (iii) $\varepsilon = 0.0000125, h = \frac{1}{32768}$.

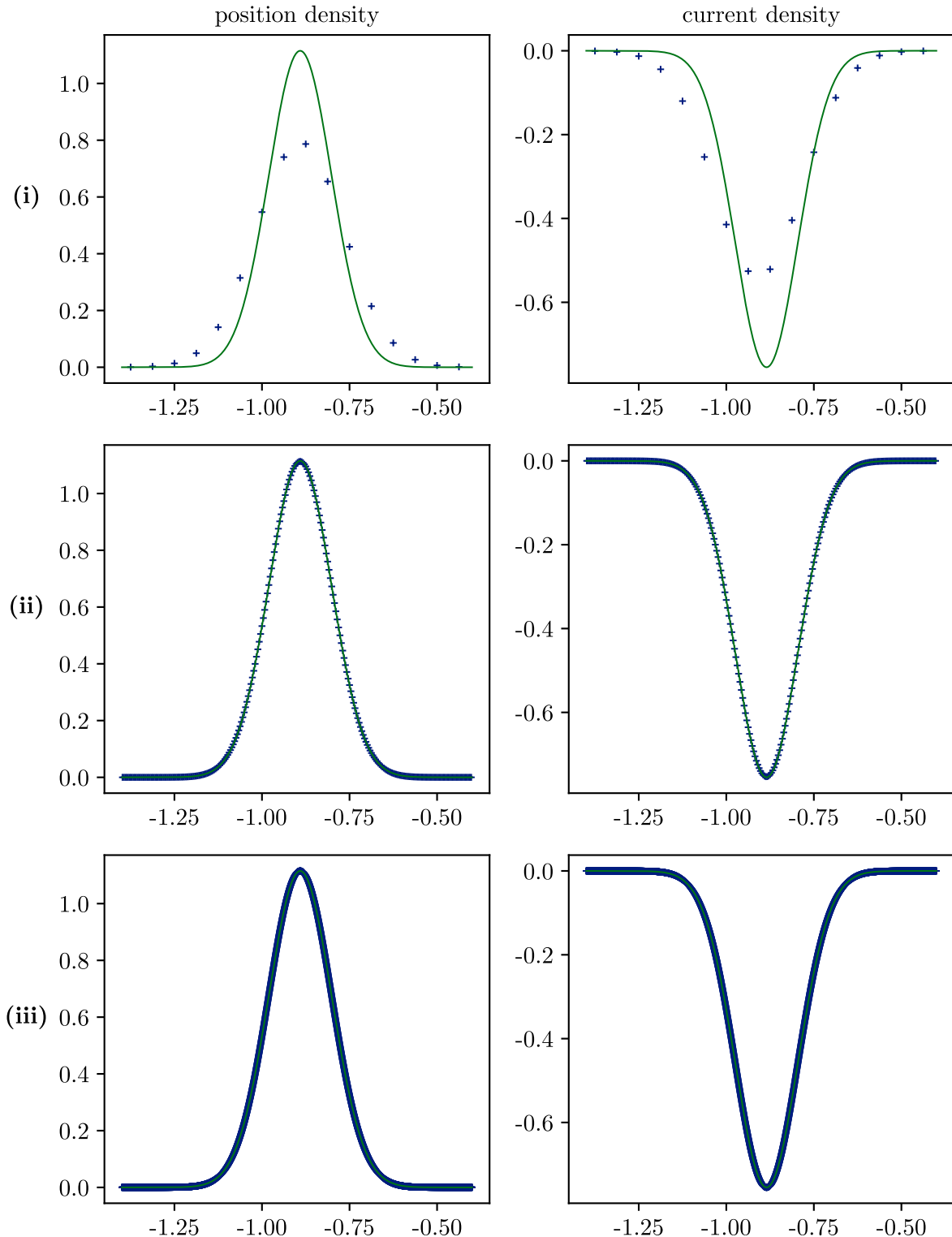


Figure 6.2: Example 2. Numerical solutions at $t = 3.6$, with time step $k = 0.05$. $\textcolor{blue}{++}$: numerical solution; $\textcolor{green}{—}$: analytical weak limit; $V(x) = x^2/2$; (i) $\varepsilon = 0.04$, $h = \frac{1}{16}$; (ii) $\varepsilon = 0.00256$, $h = \frac{1}{256}$; (iii) $\varepsilon = 0.00015625$, $h = \frac{1}{4096}$.

The problem is integrated to $T = 2.7$, with a constant time step $k = 0.05$.

See `SP2_2D` in Appendix B for the code in Python. The computational implementation is largely the same as the 1-D case. The only difficulty is that the coefficients labelled ν_n and μ_m in (5.9) require careful use of meshgrids.

The analytical solution for the position density in the $\varepsilon \rightarrow 0$ limit are given by [GM97] as

$$n(x, y, t) = \frac{1}{|\cos t|} n_0 \left(\frac{x - \sin t}{\cos t}, \frac{y - \frac{1}{2} \sin t}{\cos t} \right).$$

The plots of some cross-sections of the position density are found in Figure 6.3. We see similar behaviour to that of Example 2, as expected of the harmonic oscillator with similar initial conditions.

6.2 Experimental Order of Convergence

In Section 3.4, we investigated the experimental order of convergence for the time-splitting method for a 2×2 matrix. Here, we will perform a similar experiment for the entire time-splitting spectral method for the Schrödinger equation.

To test the dependence on the time step, a non-constant potential is needed. We will reuse the setup from Example 2 with $\varepsilon = 0.0256$ and $h = \frac{1}{32768}$ fixed. The small value of $h = \frac{b-a}{M}$ is used to make the spectral error term in (5.2) negligibly small. A final time of $T = 3.072$ is used in order to make space for more values of k .

Since we do not have an exact solution (we only have solutions in the $\varepsilon \rightarrow 0$ limit), a very fine spatial mesh size and small time step are used with the Strang splitting method as a reference, namely $h = \frac{1}{32768}$ and $k = 1 \times 10^{-5}$. We will refer to this “exact” solution as u_j , $0 \leq j \leq M$.

In this experiment, we will take a different approach to estimating the order of convergence. If the order of convergence is r , then we can assume that

$$\|u_j - U_j^N\|_{\ell^2} =: E(k) \approx Ck^r, \quad k \rightarrow 0^+$$

Taking the logarithm of both sides, we obtain the following linear relationship:

$$\log(E(k)) \approx r \log(k) + \log(C).$$

Therefore, by computing the error for several values of k , we can perform a linear regression on the data points $(\log(k), \log(E(k)))$ to obtain an estimate for r . Note that the base of the logarithm does not make a difference, as long as it is always the same base.

An interesting interpretation of the approach used to generate the EOC values in Section 3.4 is that we are taking the gradient of this log-log graph, which should give us the same EOC result.

Figure 6.4 shows the experimental data, along with the fitted curve. The orders of the methods line up with the experimental results in Section 3.4, as well as the analytical results in Section 4.3.

However, both plots demonstrate a common property of both splitting methods - the accuracy of their error estimates are highly sensitive to the size of k . This can be understood analytically due to an assumption made in Theorem 5.2, namely that $\frac{k}{\varepsilon} = \mathcal{O}(1)$. We see that for the Lie splitting method, once $k \approx 0.1 \approx 4\varepsilon$, the convergence order estimate fails. The right-hand plot shows that

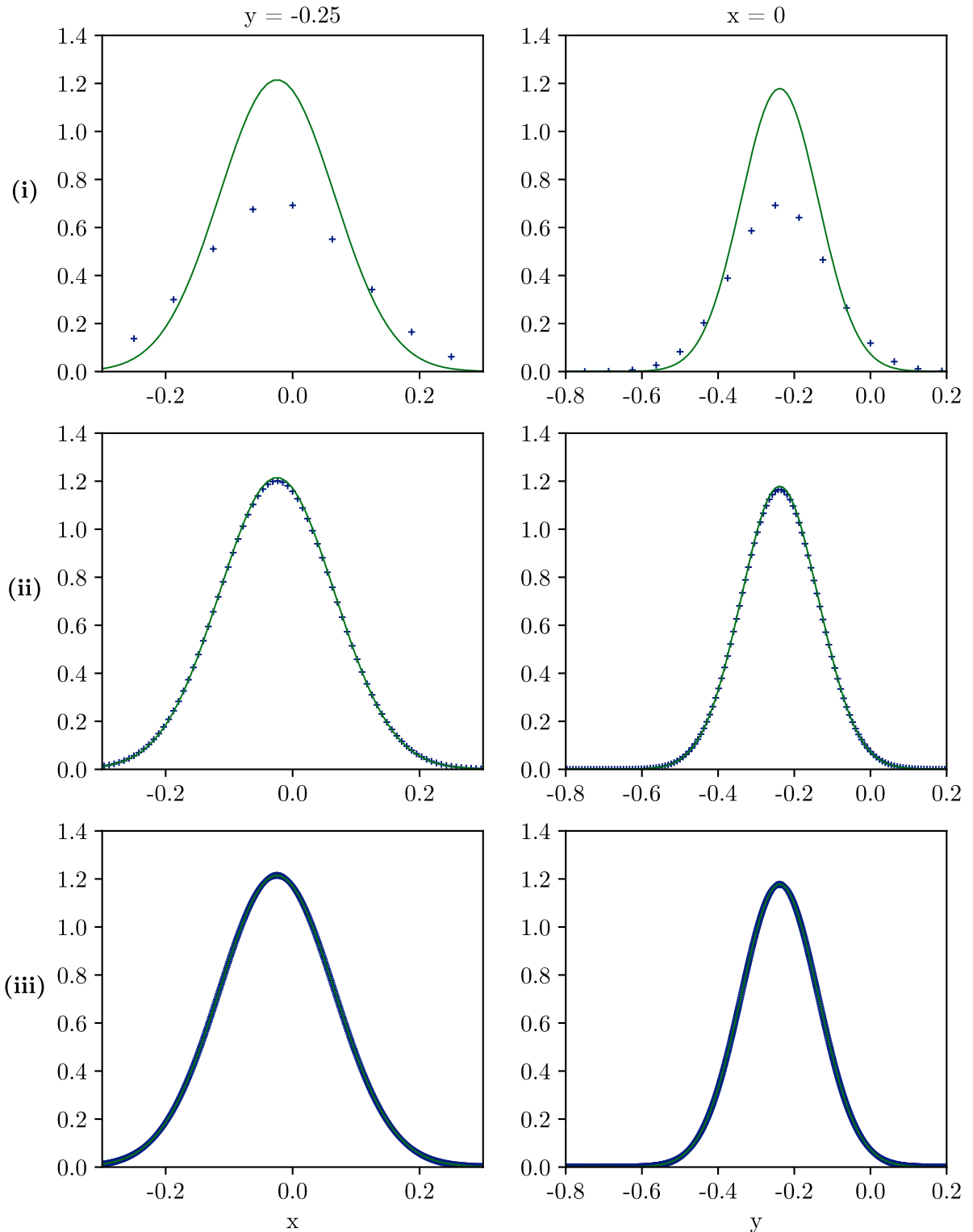


Figure 6.3: Example 3. Cross-sections of numerical solutions at $t = 2.7$. +++ : numerical solution, — : analytical weak limit; $V(x) = \frac{x^2+y^2}{2}$; (i) $\epsilon = 0.04, h = \frac{1}{16}$; (ii) $\epsilon = 0.005, h = \frac{1}{128}$; (iii) $\epsilon = 0.000625, h = \frac{1}{1024}$.

the Strang splitting method stops following its quadratic order of convergence at $k \approx 1 \approx 40\varepsilon$, which suggests a less restrictive convergence condition.

Remark 6.1. *This experimentation is not in contradiction to (5.7), since we are measuring the error of the wave function, not its observables.*

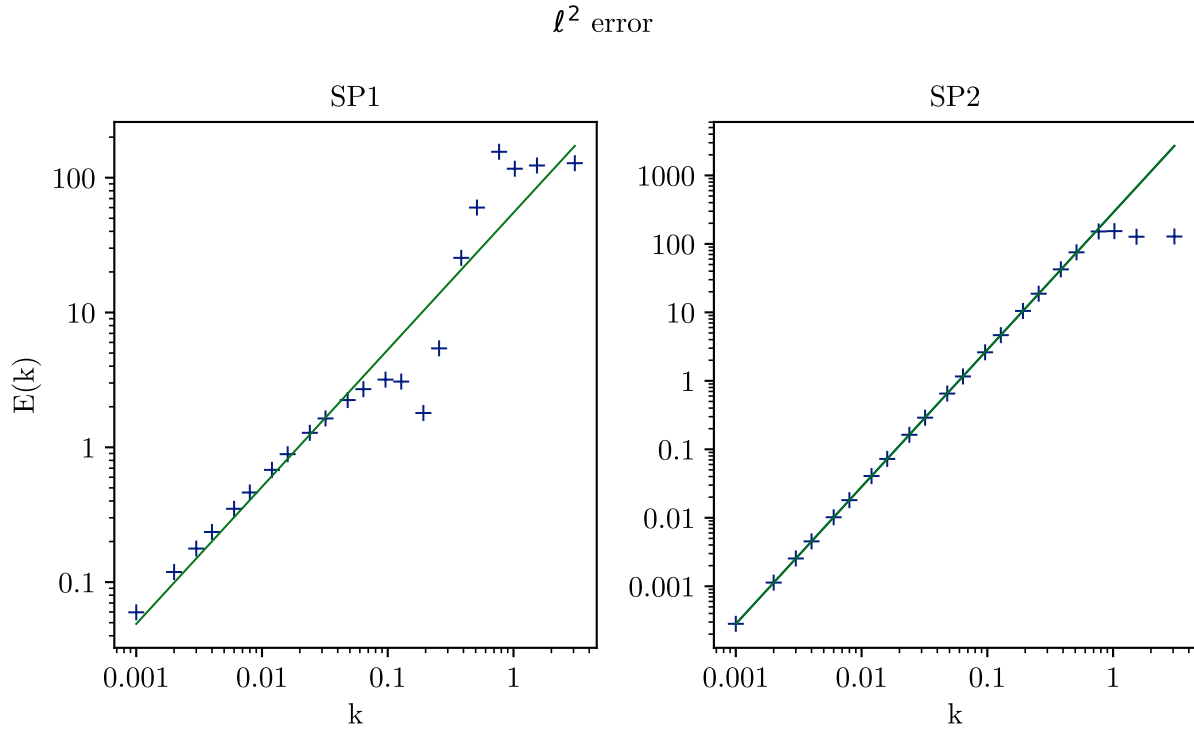


Figure 6.4: Log-log plot of error and time step size for $\varepsilon = 0.0256$. $+++$: Data points, —: linear regression; **SP1** —: $\text{Error}_2 = 55.01k^{1.02}$ **SP2** —: $\text{Error}_2 = 285.51k^{2.00}$

Chapter 7

Conclusions

This project aims to explain the methods presented in [BJM02] to an audience that is not familiar with numerical analysis, spectral methods, or quantum physics. We begin with exploring the motivation of the small-sclaed Planck constant $0 < \varepsilon \ll 1$, followed by proving a conservation of mass result.

General splitting methods for ODEs are then defined, with the Lie and Strang splitting methods being special cases. Order of convergence estimates are proved, and confirmed using computational experimentaion. We present the application of splitting methods to the Schrödinger equation in the time domain. The methods are discretized in space using a Fourier spectral method, and extended to 2-dimensions. The entire time-splitting spectral method is proved to preserve the conservation of mass law, and is therefore unconditionally stable. Furthermore, for constant potentials, the splitting error is 0, and therefore the total error scales exponentially with the spatial step.

Finally, we perform a series of numerical experiments. As per [BJM02], caustics and singularities are captured qualitatively well for $h = \mathcal{O}(\varepsilon)$. Extensions to higher numbers of spatial dimensions are trivial, and a 2-dimensional example is shown. Time-independent but non-constant potentials are shown to introduce a splitting error. However, the splitting methods allow for $h = \mathcal{O}(\varepsilon)$ and k independent of ε .

Bibliography

- [BJM02] Weizhu Bao, Shi Jin, and Peter A. Markowich. “On Time-Splitting Spectral Approximations for the Schrödinger Equation in the Semiclassical Regime”. In: *Journal of Computational Physics* 175.2 (Jan. 20, 2002), pp. 487–524. ISSN: 0021-9991. DOI: 10.1006/jcph.2001.6956.
- [BJM03] Weizhu Bao, Shi Jin, and Peter A Markowich. “Numerical study of time-splitting spectral discretizations of nonlinear Schrödinger equations in the semiclassical regimes”. In: *SIAM Journal on Scientific Computing* 25.1 (2003), pp. 27–64.
- [BT03] Weizhu Bao and Weijun Tang. “Ground-state solution of Bose–Einstein condensate by directly minimizing the energy functional”. In: *Journal of Computational Physics* 187.1 (2003), pp. 230–254. ISSN: 0021-9991. DOI: [https://doi.org/10.1016/S0021-9991\(03\)00097-4](https://doi.org/10.1016/S0021-9991(03)00097-4). URL: <https://www.sciencedirect.com/science/article/pii/S0021999103000974>.
- [Eur] European Mathematical Society. “Campbell-Hausdorff formula”. In: *Encyclopedia of Mathematics*. URL: https://encyclopediaofmath.org/wiki/Campbell-Hausdorff_formula.
- [Fra08] Jason Frank. “Numerical Analysis 2”. 2008. URL: <https://webspace.science.uu.nl/~frank011/Classes/numwisk/>.
- [GM97] Ingenuin Gasser and Peter A. Markowich. “Quantum hydrodynamics, Wigner transforms, the classical limit”. In: *Asymptotic Analysis* 14.2 (Mar. 1, 1997). Publisher: SAGE Publications, pp. 97–116. ISSN: 0921-7134. DOI: 10.3233/ASY-1997-14201.
- [Ist03] Farago Istvan. “Splitting method”. Lecture notes. Lecture notes. 2003. URL: <https://faragois.web.elte.hu//phdcourse/lecturefi2.pdf>.
- [Leo10] Ulf Leonhardt. *Essential quantum optics: from quantum measurements to black holes*. Cambridge University Press, 2010.
- [Luc24] Dan Lucas. “MT4112 Computational Numerical Analysis”. Lecture notes. 2024.
- [MMP94] P. A. Markowich, N. J. Mauser, and F. Poupaud. “A Wigner-function approach to (semi)classical limits: Electrons in a periodic potential”. In: *Journal of Mathematical Physics* 35.3 (Mar. 1, 1994), pp. 1066–1094. ISSN: 0022-2488. DOI: 10.1063/1.530629.
- [MPP99] Peter A Markowich, Paola Pietra, and Carsten Pohl. “Numerical approximation of quadratic observables of Schrödinger-type equations in the semi-classical limit”. In: *Numerische Mathematik* 81 (1999), pp. 595–630.
- [Wil24] Antonia Wilmot-Smith. “MT4511 Asymptotic Methods”. Lecture notes. 2024.

Appendix A

Mathematical derivations

A.1 An approach to the semi-classical scaling

In the Section 2.1, it is stated that certain limits of x and/or t are equivalent to converting from the TDSE (2.1) to the semi-classical Schrödinger equation (2.2). This will be explored in more detail.

Consider the time-independent Schrödinger equation with a time-independent potential

$$\frac{\hbar^2}{2m} \frac{\partial^2 \psi}{\partial x^2} + i\hbar \frac{\partial \psi}{\partial t} - V(x)\psi = 0.$$

The potential is kept time-independent since that is the only type of potential we are investigating in this project.

Let us rescale the time and space variables as follows.

$$x = Lx', \quad \text{and} \quad t = \frac{L}{v_0}t',$$

for L a length scaling constant, and v_0 a velocity scaling constant. Note that these constants will absorb the dimensions of the original x and t variables, resulting in dimensionless variables x' and t' .

We get the following transformations

$$\begin{aligned} \frac{\partial^2 \psi}{\partial x^2} &= \frac{1}{L^2} \frac{\partial^2 \psi}{\partial x'^2} \\ \frac{\partial \psi}{\partial t} &= \frac{v_0}{L} \frac{\partial \psi}{\partial t'}. \end{aligned}$$

Now, substituting in, dropping the primes, and simplifying,

$$\begin{aligned} \frac{\hbar^2}{2m} \frac{1}{L^2} \frac{\partial^2 \psi}{\partial x^2} + i\hbar \frac{v_0}{L} \frac{\partial \psi}{\partial t} - V(Lx)\psi &= 0 \\ \frac{\hbar^2}{2mLv_0} \frac{\partial^2 \psi}{\partial x^2} + i\hbar \frac{\partial \psi}{\partial t} - \frac{L}{v_0} V(Lx)\psi &= 0. \end{aligned}$$

Motivated by the $\frac{\hbar^2}{2mLv_0}$ term in front of the second derivative, set $\hbar = \varepsilon m Lv_0$ for a real constant ε .

$$\begin{aligned} \frac{\varepsilon^2 m Lv_0}{2} \frac{\partial^2 \psi}{\partial x^2} + i\varepsilon m Lv_0 \frac{\partial \psi}{\partial t} - \frac{L}{v_0} V(Lx) \psi &= 0 \\ \frac{\varepsilon^2}{2} \frac{\partial^2 \psi}{\partial x^2} + i\varepsilon \frac{\partial \psi}{\partial t} - \frac{1}{mv_0^2} V(Lx) \psi &= 0. \end{aligned}$$

This equation looks almost like the semi-classical Schrödinger equation (2.2) we are looking for. However, we have conveniently ignored the buildup of terms in front of, and inside, our potential term. The constant in front is easy to absorb into the potential: letting $V = mv_0^2 V'$, we obtain a dimensionless potential V' , due to the fact that the units of the potential (and the entirety of the TDSE) are of energy.

However, the factor of L in the potential is worrying, since we have no information about the functional form of V . This dependence on L must be dealt with on a case-by-case basis. See Section 2.1 in [BT03] for an example related to the Gross-Pitaevskii equation.

Therefore, replacing $V(Lx)$ with $V(x)$, we recover the time-dependent Schrödinger equation in the semi-classical regime

$$\frac{\varepsilon^2}{2} \frac{\partial^2 \psi}{\partial x^2} + i\varepsilon \frac{\partial \psi}{\partial t} - V(x) \psi = 0.$$

A.2 Wigner functions and the free particle problem

In Section 6.1, Example 1 presents a particle in a constant potential $V(x, t) = V_0 \equiv 10$, which is also called a free particle, since $\nabla V \equiv 0$.

This example is notable because the initial condition results in *caustics* forming when characteristic lines intersect. We will investigate the analytical solution to this here.

We define the Wigner function of a wave function $u^\varepsilon(x, t)$ as

$$w^\varepsilon(x, v, t) = \frac{1}{2\pi} \int_{-\infty}^{\infty} \overline{u^\varepsilon}(x + \varepsilon \frac{\eta}{2}, t) u^\varepsilon(x - \varepsilon \frac{\eta}{2}, t) e^{iv \cdot \eta} d\eta.$$

This function has the property that its v -moments yield certain observables. Namely, the zeroth moment gives the position density,

$$n^\varepsilon(x, t) = \int_{-\infty}^{\infty} w^\varepsilon(x, v, t) dv$$

and the first moment gives the current density,

$$J^\varepsilon(x, t) = \int_{-\infty}^{\infty} v w^\varepsilon(x, v, t) dv.$$

Furthermore, the Wigner function satisfies the following evolution equation [GM97]:

$$\frac{\partial w^\varepsilon}{\partial t} + v \cdot \frac{\partial w^\varepsilon}{\partial x} - \theta[V]w^\varepsilon = 0 \quad (\text{A.1})$$

for $\theta[V]$ a pseudo-differential operator with the property $\nabla V = 0 \Rightarrow \theta[V] = 0$.

See [Leo10, Chapter 4] for a textbook explanation of Wigner functions, and [MMP94] and [GM97] for more in-depth examples of Wigner functions applied to the semi-classical Schrödinger equation. For our purposes, these results are enough to solve the following problem.

Let u^ε be such that

$$i\varepsilon \frac{\partial u^\varepsilon}{\partial t} + \frac{\varepsilon^2}{2} \frac{\partial^2 u^\varepsilon}{\partial x^2} - V(x)u^\varepsilon = 0,$$

with initial condition of the Wentzel-Kramers-Brillouin (WKB) form

$$u^\varepsilon(x, t=0) = u_I^\varepsilon(x) = \sqrt{n_I(x)} e^{iS_I(x)/\varepsilon}$$

for

$$n_I(x) = e^{-50(x-0.5)^2} \quad \text{and} \quad S_I(x) = \frac{1}{5} \ln \left(e^{5(x-0.5)} + e^{-5(x-0.5)} \right).$$

Then, for the *classical limit* $\varepsilon \rightarrow 0$, find

$$n^0(x, t) := \lim_{\varepsilon \rightarrow 0} n^\varepsilon(x, t) \quad \text{and} \quad J^0(x, t) := \lim_{\varepsilon \rightarrow 0} J^\varepsilon(x, t).$$

Now, we have that the initial condition for (A.1) is

$$\begin{aligned} w_I^\varepsilon(x, v) &= \frac{1}{2\pi} \int_{-\infty}^{\infty} \overline{u_I}(x + \varepsilon \frac{\eta}{2}) u_I(x - \varepsilon \frac{\eta}{2}) e^{iv \cdot \eta} d\eta \\ &= \frac{1}{2\pi} \int_{-\infty}^{\infty} \sqrt{n_I(x + \varepsilon \frac{\eta}{2}) n_I(x - \varepsilon \frac{\eta}{2})} e^{-\frac{i}{\varepsilon} [S_I(x + \eta \frac{\varepsilon}{2}) - S_I(x - \eta \frac{\varepsilon}{2})]} e^{iv \cdot \eta} d\eta \end{aligned}$$

taking $\varepsilon \rightarrow 0$, and by definition of the derivative, we get

$$\begin{aligned} w_I^0(x, v) &= n_I(x) \frac{1}{2\pi} \int_{-\infty}^{\infty} e^{-i \frac{d}{dx} S_I(x) \cdot \eta} e^{iv \cdot \eta} d\eta \\ &= n_I(x) \frac{1}{2\pi} \int_{-\infty}^{\infty} e^{[v - i \frac{d}{dx} S_I(x)] \cdot i\eta} d\eta \end{aligned}$$

and so, by the well-known identity

$$\int_{-\infty}^{\infty} e^{i\eta x} d\eta = 2\pi \delta(x),$$

we obtain the initial condition of the Wigner function for $\varepsilon \rightarrow 0$, as given by Equation 5.4b in [MPP99]

$$w_I^0(x, v) = n_I(x) \delta \left(v - \frac{d}{dx} S_I(x) \right).$$

Now, noting that $\frac{dV}{dx} = 0$, (A.1) simplifies to the one-dimensional advection equation

$$\frac{\partial w^0}{\partial t} + v \cdot \frac{\partial w^0}{\partial x} = 0. \quad (\text{A.2})$$

We notice that along characteristic lines $x = vt + x_0$, w^0 is constant, and is equal to $w_I^0(x_0, v) = w_I^0(x - vt, v)$. Therefore, we have that the solution to (A.2) is

$$w^0(x, v, t) = w_I^0(x - vt, v).$$

Finally, we can solve for the v -moments n^0 and J^0 . First, note that

$$\frac{d}{dx} S_I(x) = -\tanh(5(x - 0.5))$$

and so, let $\mu_v^n(x, t)$ be the n th v -moment of $w^0(x, v, t)$.

$$\begin{aligned} \mu_v^n(x, t) &= \int_{-\infty}^{\infty} v^n w^0(x, v, t) dv \\ &= \int_{-\infty}^{\infty} v^n n_I(x - vt) \delta(v + \tanh[5(x - vt - 0.5)]) dv. \end{aligned}$$

Let $s = h(v) = v + \tanh(5(x - vt - 0.5))$ for constant x, t such that $ds = h'(v) dv$. Note that $h(v)$ is not monotone for $t > 0.2$, which means that $h^{-1}(v)$ can have multiple roots for some values of x and t . Therefore, the delta function will have multiple contributions at multi-valued points. So, by definition of $\delta(g(x)) = \sum_{x_i: g(x_i)=0} \frac{\delta(x - x_i)}{|g'(x_i)|}$

$$\mu_v^n(x, t) = \int_{-\infty}^{\infty} v^n n_I(x - vt) \sum_{v_i: h(v_i)=0} \frac{\delta(v - v_i)}{|h'(v_i)|} dv = \sum_{v: h(v)=0} \frac{v^n n_I(x - vt)}{h'(v)}.$$

The position and current density are the zeroth and first moment respectively, so

$$n^0(x, t) = \sum_{v: h(v)=0} \frac{n_I(x - vt)}{h'(v)} \quad \text{and} \quad J^0(x, t) = \sum_{v: h(v)=0} \frac{vn_I(x - vt)}{h'(v)}. \quad (\text{A.3})$$

This form of the solution is only as useful as it is easy to find the roots of h . Since $\tanh(x) \in (-1, 1)$ for all $x \in \mathbb{R}$, the solutions to $h(v) = 0 \Rightarrow v = -\tanh(f(v))$ must also be in $(-1, 1)$. This allows

the computational implementation to be quite simple, since the range to look over is bounded and fixed.

The plots of $n^0(x, t)$ and $J^0(x, t)$ in Figure A.1 reveal caustics for $t \geq 0.2$. These caustics are singular points of the observables, marking the transition where the characteristics of the Wigner function $w^0(x, v, t)$ change behavior: outside the caustics, $h(v) = v + \tanh(5(x - vt - 0.5))$ has one root (no intersection of characteristics), while between the caustics, $h(v)$ has three roots (a three-fold intersection of characteristics).

Note that this is conditioned on $t > 0.2$ because

$$\frac{\partial h}{\partial v} = 1 - 5t \operatorname{sech}^2(5(x - vt - 0.5)) \quad \text{and} \quad \max_{y \in \mathbb{R}} \operatorname{sech}(y) = \operatorname{sech}(0) = 1,$$

so $h(v)$ can have more than 0 turning points for some x iff $5t \geq 1 \Rightarrow t \geq 0.2$.

Remark A.1. *Since v is dependent on x and t , the characteristic lines of the advection equation (A.2) are able to intersect. This is not the case for the usual one-dimensional advection equation because v is constant.*

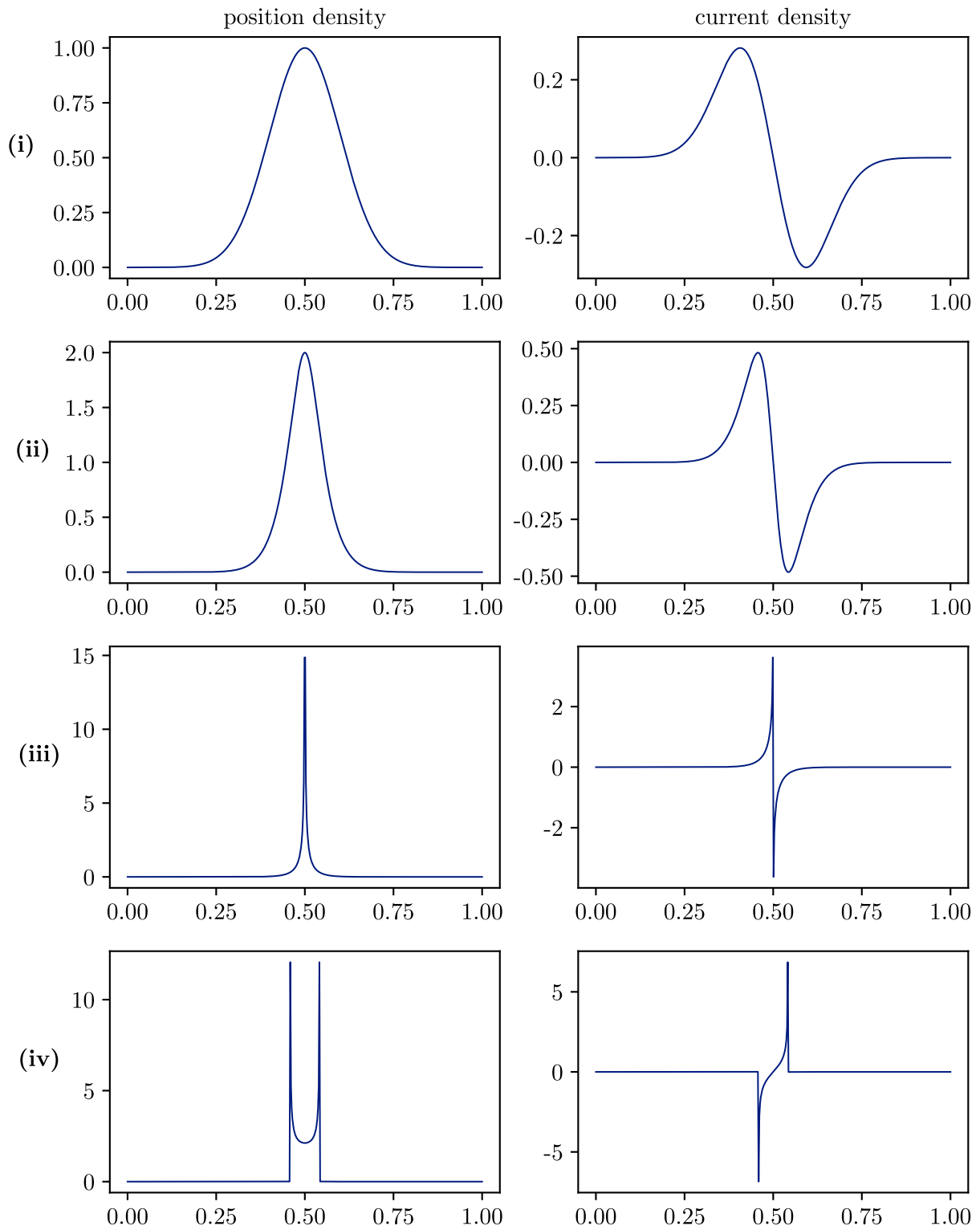


Figure A.1: Plots at various times of the analytical solution of the observables. Free particle potential $V(x) = 10$; (i) $t = 0$; (ii) $t = 0.1$, before caustics form; (iii) $t = 0.2$, when caustics form; (iv) $t = 0.3$, after caustics form;

Appendix B

Computational implementation

B.1 Main functions

These are the functions that are used throughout the project, most importantly the implementations of the time-splitting spectral methods.

Listing B.1: 1-dimensional Lie splitting method (SP1)

```
def SP1(u0, a, b, T, h, k, eps, V):
    xarr = np.arange(a, b, h)
    #  $T+k/2$  is the end so that  $T$  is the last element
    tarr = np.arange(0, T + k/2, k)
    u = u0
    n = len(u)

    mu = np.fft.freq(n, h) * 2 * np.pi
    # tqdm is a light-weight progress bar
    for _ in tqdm(tarr[1:]):
        uhat = np.fft.fft(u)

        # first step: finding  $U^*$  from  $U^n$ 
        uhat *= np.exp(-0.5j*eps*k*mu**2)
        ustard = np.fft.ifft(uhat)

        # second step: finding  $U^{n+1}$  from  $U^*$ 
        u = np.exp(-1j * k / eps * V(xarr, _)) * ustard

    return u # only returns the last element
```

Listing B.2: 1-dimensional Strang splitting method (SP2)

```
def SP2(u0, a, b, T, h, k, eps, V):
    xarr = np.arange(a, b, h)
    #  $T+k/2$  is the end so that  $T$  is the last element
    tarr = np.arange(0, T + k/2, k)
    u = u0
```

```

n = len(u)

mu = np.fft.fftfreq(n, h) * 2 * np.pi
V_mult = np.exp(-0.5j * k / eps * V(xarr, tarr))
laplace_mult = np.exp(-0.5j * eps * k * mu**2)

for _ in tqdm(tarr[1:]):
    # first step: U^* from U^n
    ustar1 = V_mult * u

    # second step: U^{**} from U^*
    uhat = laplace_mult * np.fft.fft(ustar1)
    ustar2 = np.fft.ifft(uhat)

    # third step: finding U^{n+1} from U^{**}
    u = V_mult * ustar2

return u

```

Listing B.3: 2-dimensional Strang splitting method (SP2)

```

def SP2_2D(u0, xgrid, ygrid, T, hx, hy, k, eps, V):
    tarr = np.arange(0, T+k/2, k)
    u = u0
    nx, ny = xgrid.shape

    # precomputing laplace and potential multipliers
    mux = np.fft.fftfreq(nx, hx) * 2 * np.pi
    muy = np.fft.fftfreq(ny, hy) * 2 * np.pi
    mux_grid, muy_grid = np.meshgrid(mux, muy)
    mu_laplace_grid = (mux_grid**2 + muy_grid**2)

    laplace_mult = np.exp(-0.5j * eps * k * mu_laplace_grid)
    V_mult = np.exp(-0.5j * k / eps * V(xgrid, ygrid, 0))

    for _ in tqdm(tarr[1:]):
        # U^n -> U^*
        ustar1 = V_mult * u

        # U^* -> U^{**}
        uhat = np.fft.fft2(ustar1)
        uhat *= laplace_mult
        ustar2 = np.fft.ifft2(uhat)

        # U^{**} -> U^{n+1}
        u = V_mult * ustar2

    return u

```

Listing B.4: Current and position density

```
# spectral differentiation for the computation of the current density
def diff(y, dx, ord, axis=-1):
    n = y.shape[axis]
    # Scaled frequencies (angular frequency)
    k = np.fft.fftfreq(n, d=dx) * 2 * np.pi

    # Compute the FFT of the function
    y_hat = np.fft.fft(y, axis=axis)
    # Scale by (i*k)^ord to compute the derivative in Fourier space
    dy_hat = (1j * k) ** ord * y_hat

    # Transform back to real space
    return np.fft.ifft(dy_hat, n=n, axis=axis)

def curr_density(u, eps, dx):
    grad_u = diff(u, dx, 1, -1)
    return eps*np.imag(np.conjugate(u)*grad_u)

def pos_density(u):
    return np.abs(u)**2
```

B.2 Experiments

This is the stripped-down version of the code used to generate the examples in Section 6.1, and the experimental order of convergence data in Section 6.2. Many of the plotting functions have been removed for brevity.

Listing B.5: Splitting method applied to Example 1

```
# initial condition
def n_0(x):
    a = -25 * (x - 0.5)**2
    return np.exp(a)**2

def S_0(x):
    a = np.exp(5 * (x - 0.5))
    return -0.2 * np.log(a + 1/a)

def u0(x, eps):
    return np.sqrt(n_0(x)) * np.exp(1j * S_0(x) / eps)

# epsilon and h values for each plot.
eps_vals = [0.0064, 0.0001, 0.0000125]
h_vals = [1/64, 1/4096, 1/32768]

def V(x, t):
    return 10
```

```

T = 0.54
for i, (eps, h) in enumerate(zip(eps_vals, h_vals)):
    xarr = np.arange(0, 1, h)
    tarr = np.arange(0, 1.1*T, T)
    # k = T so it's only one step
    uarr = SP2(u0(xarr, eps), 0, 1, T, h, T, eps, V)

pd = pos_density(uarr)
cd = curr_density(uarr, eps, h)

```

Listing B.6: Computation of the weak limit for Example 1, as per (A.3)

```

def dh(x, v, t):
    sech2 = (np.cosh(5*(x - v*t - 0.5)))**(-2)
    return 1 - 5*t*sech2

def h(x, v, t):
    return v + np.tanh(5*(x - v*t - 0.5))

def find_roots(x, t, v_range, num_guesses=100):
    # univariate function for root
    def univariate_h(v):
        return h(x, v, t)
    def univariate_dh(v):
        return dh(x, v, t)
    roots = []

    v_guesses = np.linspace(*v_range, 10)

    for v0 in v_guesses:
        sol = root(univariate_h, v0)
        if sol.success:
            v_root = sol.x[0]
            if not any(np.isclose(v_root, r) for r in roots):
                roots.append(v_root)
                if np.abs(v_root) > 1:
                    print("WARNING: abs(root) > 1")
        if len(roots) >= 3:
            break

    if len(roots) not in (1, 3):
        print(f"WARNING: only {len(roots)} roots")
    return roots

def compute_n(x, t, v_range=(-1, 1)):
    roots = find_roots(x, t, v_range)
    n0_vals = []
    for v in roots:

```

```

deriv = np.abs(dh(x, v, t))
deriv = max(deriv, 1e-6) # avoid divide by 0
if np.abs(deriv) < 1e-6:
    deriv = 1e-6
n = n_0(x - v*t) / deriv
n0_vals.append(n)

n0 = sum(n0_vals)
return n0

def compute_J(x, t, v_range=(-1, 2)):
    roots = find_roots(x, t, v_range)
    n0_vals = []
    for v in roots:
        dh_0 = np.abs(dh(x, v, t))
        if np.abs(dh_0) < 1e-6:
            dh_0 = 1e-6
        n = v*n_0(x - v*t) / dh_0
        n0_vals.append(n)

    n0 = sum(n0_vals)
    return n0

```

The code for the other examples is not included, since the implementation is largely the same, and the analytical solutions are explicit.

Listing B.7: Order of convergence in k experiment in Section 6.2.

$T = 3.072$

```

eps_vals = [0.0256]
k_vals = [0.001, 0.002, 0.003, 0.004, 0.006, 0.008, 0.012, 0.016, 0.024,
          0.032, 0.048, 0.064, 0.096, 0.128, 0.192, 0.256, 0.384, 0.512,
          0.768, 1.024, 1.536, 3.072]

# 2 in first axis to store SP1 and SP2 data
results = np.zeros((2, len(eps_vals), len(k_vals)))

h = 1./32768
a, b = -2, 2

xarr = np.arange(a, b, h)
k_exact = 1e-5

for i, eps in enumerate(eps_vals):
    # the following line took a very long time to run - in practice,
    # outputs were pickled and stored.
    exact_sol = SP2(u0(xarr, eps), a, b, T, h, k_exact, eps, V)

```

```
for j , k in enumerate(k_vals):
    print(f"eps = {eps:.5f}, k = {k:.5f}")
    print("computing SP1 approximation ...")
    sp1_uarr = SP1(u0(xarr, eps), a, b, T, h, k, eps, V)
    print("computing SP2 approximation ...")
    sp2_uarr = SP2(u0(xarr, eps), a, b, T, h, k, eps, V)

    results[0, i, j] = np.linalg.norm(sp1_uarr - exact_sol, ord=2)
    results[1, i, j] = np.linalg.norm(sp2_uarr - exact_sol, ord=2)
```